REPORT DOCUMENTATION PAGE

Form Approved OMB NO. 0704-0188

1. REPORT DATE (DD-MM-YYYY)	2. REPORT TYPE	3. DATES COVERED (From - To)
01-03-2019	Final Report	18-Jun-2012 - 17-Oct-2015

4. TITLE AND SUBTITLE
Final Report: Organic Matrix Templating and Function in an Ultrahard Biological Composite

5a. CONTRACT NUMBER
W911NF-12-1-0257

5b. GRANT NUMBER

5c. PROGRAM ELEMENT NUMBER
611102

5d. PROJECT NUMBER

5e. TASK NUMBER

5f. WORK UNIT NUMBER

6. AUTHORS

7. PERFORMING ORGANIZATION NAMES AND ADDRESSES
University of California - Riverside
200 University Office Building

Riverside, CA 92521 -0001

8. PERFORMING ORGANIZATION REPORT NUMBER

9. SPONSORING/MONITORING AGENCY NAME(S) AND ADDRESS (ES)
U.S. Army Research Office
P.O. Box 12211
Research Triangle Park, NC 27709-2211

10. SPONSOR/MONITOR'S ACRONYM(S)
ARO

11. SPONSOR/MONITOR'S REPORT NUMBER(S)
61843-LS-H.4

12. DISTRIBUTION AVAILIBILITY STATEMENT
Approved for public release; distribution is unlimited.

13. SUPPLEMENTARY NOTES
The views, opinions and/or findings contained in this report are those of the author(s) and should not contrued as an official Department of the Army position, policy or decision, unless so designated by other documentation.

14. ABSTRACT

15. SUBJECT TERMS

16. SECURITY CLASSIFICATION OF: a. REPORT	b. ABSTRACT	c. THIS PAGE	17. LIMITATION OF ABSTRACT	15. NUMBER OF PAGES	19a. NAME OF RESPONSIBLE PERSON / 19b. TELEPHONE NUMBER
UU	UU	UU	UU		David Kisailus / 951-827-4310

Standard Form 298 (Rev 8/98)
Prescribed by ANSI Std. Z39.18

RPPR Final Report
as of 08-May-2019

Agency Code:

Proposal Number: 61843LSH **Agreement Number: W911NF-12-1-0257**

INVESTIGATOR(S):

Name: David Kisailus
Email: kisailus@ucr.edu
Phone Number: 9518274310
Principal: Y

Organization: **University of California - Riverside**
Address: 200 University Office Building, Riverside, CA 925210001
Country: USA

DUNS Number: 627797426 EIN: 956006142
Report Date: 17-Jan-2016 Date Received: 01-Mar-2019
Final Report for Period Beginning 18-Jun-2012 and Ending 17-Oct-2015
Title: Organic Matrix Templating and Function in an Ultrahard Biological Composite
Begin Performance Period: 18-Jun-2012 **End Performance Period:** 17-Oct-2015
Report Term: 0-Other

Submitted By: David Kisailus Email: kisailus@ucr.edu
Phone: (951) 827-4310

Distribution Statement: 1-Approved for public release; distribution is unlimited.

STEM Degrees: **STEM Participants:**

Major Goals: Overall objectives

The long-term objective of this project was to understand the mechanisms of nanostructural development in mineralizing environments and relate them to creating hierarchical nanostructures that afford impressive functional properties, specifically in unique abrasion resistant and damage-tolerant composites. The progress from this work will enable the development of the necessary tools for the design and fabrication of cost-effective and environmentally friendly engineering materials that mimic key design elements and performance properties present in biological systems.
We achieved this by investigating the underlying organics that direct the nucleation and fine-tuned growth of mineral using modern spectroscopic and microscopic characterization techniques. Specifically, we performed (i) a detailed study of the chemical and ultrastructural features of the fully mineralized radular teeth in Cryptochiton stelleri with a complementary mechanical investigation (combined modeling and experimental) of the mineralized structures, (ii) a thorough investigation of the underlying organic framework (structural and chemical) that provides templating for mineral growth as well as scaffolding for the teeth, (iii) synthesis of biomimetic materials through in-vitro mineralization studies to understand organic-inorganic interactions and growth mechanisms that provide architectural features that enhance abrasion resistance and damage tolerance.

Specific objectives:

1. Investigation of chemical and ultrastructural features of the fully mineralized radular teeth in Cryptochiton stelleri (chiton) with a complementary mechanical investigation of the mineralized structures.

2. Thorough investigation of the underlying organic framework (structural and chemical) that provides templating for mineral growth as well as scaffolding for the teeth

3. Synthesis of biomimetic materials

Accomplishments: Please see uploaded document with all details of accomplishments.

Training Opportunities: Please see uploaded document for details.

Results Dissemination: Please see uploaded document for details.

Honors and Awards: Please see uploaded document for details.

Protocol Activity Status:

Technology Transfer: Please see uploaded document for details.

PARTICIPANTS:

Participant Type: PD/PI
Participant: David Kisailus
Person Months Worked: 3.00 **Funding Support:**
Project Contribution:
International Collaboration:
International Travel:
National Academy Member: N
Other Collaborators:

Participant Type: Postdoctoral (scholar, fellow or other postdoctoral position)
Participant: Lessa Grunenfelder
Person Months Worked: 6.00 **Funding Support:**
Project Contribution:
International Collaboration:
International Travel:
National Academy Member: N
Other Collaborators:

Participant Type: Graduate Student (research assistant)
Participant: Steven Herrera
Person Months Worked: 12.00 **Funding Support:**
Project Contribution:
International Collaboration:
International Travel:
National Academy Member: N
Other Collaborators:

Participant Type: Undergraduate Student
Participant: Jeff Geiger
Person Months Worked: 6.00 **Funding Support:**
Project Contribution:
International Collaboration:
International Travel:
National Academy Member: N
Other Collaborators:

ARTICLES:

Publication Type: Journal Article Peer Reviewed: Y **Publication Status:** 1-Published
Journal: Advanced Functional Materials
Publication Identifier Type: DOI Publication Identifier: 10.1002/adfm.201202894
Volume: 23 Issue: 23 First Page #: 2809
Date Submitted: Date Published:
Publication Location:
Article Title: Phase Transformations and Structural Developments in the Radular Teeth of Cryptochiton stelleri
Authors:
Keywords: Biological composite, crystallization, organic templating
Abstract: During mineralization, the hard outer magnetic-containing shell of the radular teeth of Cryptochiton stelleri undergoes four distinct stages of structural and phase transformations: (i) the formation of a crystalline alpha-chitin organic matrix that forms the structural framework of the non-mineralized teeth (as described by Towe and Lownstam), (ii) the templated synthesis of ferrihydrite crystal aggregates along these organic fibers, (iii) subsequent solid state phase transformation from ferrihydrite to magnetite, and (iv) progressive magnetite crystal growth to form continuous parallel rods within the mature teeth. The underlying alpha-chitin organic matrix appears to influence magnetite crystal aggregate density and the diameter and curvature of the resulting rods, both of which likely play critical roles in determining the local mechanical properties of the mature radular teeth.
Distribution Statement: 1-Approved for public release; distribution is unlimited.
Acknowledged Federal Support:

Publication Type: Journal Article Peer Reviewed: Y **Publication Status:** 1-Published
Journal: PROTEOMICS
Publication Identifier Type: DOI Publication Identifier: 10.1002/pmic.201100473
Volume: 12 Issue: 18 First Page #: 2890
Date Submitted: Date Published:
Publication Location:
Article Title: Proteomic analysis from the mineralized radular teeth of the giant Pacific chiton, Cryptochiton stelleri (Mollusca)
Authors:
Keywords: Animal proteomics;Biomineralization;De novo peptide sequencing;Radular teeth
Abstract: The biomineralized radular teeth of chitons are known to consist of iron-based magnetic crystals, associated with the maximum hardness and stiffness of any biomineral. Based on our transmission electron microscopy analysis of partially mineralized teeth, we suggest that the organic matrix within the teeth controls the iron oxide nucleation. Thus, we used Nano-LC-MS to perform a proteomic analysis of the organic matrix in radular teeth of the chiton Cryptochiton stelleri in order to identify the proteins involved in the biomineralization process. Since the genome sequence of C. stelleri is not available, cross-species similarity searching and de novo peptide sequencing were used to screen the proteins. Our results indicate that several proteins were dominant in the mineralized part of the radular teeth, amongst which, myoglobin and a highly acidic peptide were identified as possibly involved in the biomineralization process.
Distribution Statement: 1-Approved for public release; distribution is unlimited.
Acknowledged Federal Support:

Final Report (2015)

<u>Organic Matrix Templating and Function in an Ultrahard Biological Composite</u>
Agreement Number W911NF-12-1-0257

PI: David Kisailus, UC Riverside

<u>Abstract</u>
Based on the three years of this project, we have been largely successful in staying on schedule and achieving the milestones outlined in the proposal. The research goal of this project was to investigate the underlying organics that direct the nucleation and fine-tuned growth of mineral using modern spectroscopic and microscopic characterization techniques to understand the mechanisms of nanostructural development to create hierarchical nanostructures that afford impressive functional properties. This will enable the development of the necessary tools for the design and fabrication of cost-effective and environmentally friendly engineering materials that mimic key design elements and performance properties present in biological systems.

During the course of this project, we have shown that the fully mineralized teeth consist of an overall core-shell structure, with the core consisting of an organic (i.e., alpha-chitin) rich iron phosphate (phosphosiderite) surrounded by a highly mineralized shell of oriented magnetite nanorods. We also determined a number of ultrastructural features within the fully mineralized tooth shell that are analogous to another well known biocomposite, the nacreous layer to the abalone shell. These include anisotropic rods that have nanoasperities and mineral bridges as well as organic, which hold these rods together under strain. We also found an outer perimeter of the tooth consisting of a thin particulate layer that may redistribute stress during rasping. Complementary mechanical investigations of these mineralized structures have revealed that in transverse section, the tooth demonstrates graded hardness and modulus. The leading edge of the tooth displays a higher hardness and modulus than the trailing edge, and is due to the difference in diameters of the nanorods. Specifically, the nanorods with a higher aspect ratio found on the leading edge were more abrasion resistant than those on the trailing edge, which were broader in diameter to reduce buckling under compression. We also investigated the partially mineralized teeth, and found that they consisted of a network of organic fibrils of alpha-chitin that were spaced similarly to the diameter of the nanorods in the fully mineralized teeth. TEM observations, in combination with synchrotron x-ray experiments revealed that the organic fibrils templated the nucleation and growth of mineral (ferrihydrite), which subsequently transformed to magnetite via solid-state transformation. The spacing of these organic templates regulated the final diameter of the magnetite nanorods, which controlled the mechanical properties of the teeth. We also investigated the interface between the teeth and the radula as well as the radular base/stylus in *Cryptochiton stelleri*. Results have shown that even before the partially mineralized teeth form, proteins (of unknown composition currently) begin to build in the radular belt and in the stylus. This may indicate specific proteins are localized within regions of the stylus/tooth to stabilize amorphous mineral precursors as well as nucleate ferrihydrite within the teeth. Chemical and complementary mechanical investigations at the interfaces between partially mineralized teeth and the styli reveal that these interfaces may act as a temporary barrier to mineral transport to the core of the tooth. In this sense, we believe there is an ion-gated process to enable phosphate ions to be transported into the core of the teeth. In addition, we made initial microscopic and

spectroscopic observations to show that the organic fibrils that make up the stylus contain regional differences in sulfur, which may provide local stiffening to support the teeth. We also observed that these fibers from the stylus continue into the tooth itself, likely providing not only a continuous structure from which momentum can be transferred, but also a path for mineral to be transported during tooth formation. We initiated development of biomimetic structures based on the architectures uncovered from ultrastructural observations made throughout this project. Specifically, we have utilized a membrane with controlled pore diameters similar to the diameters of the nanorods. We have demonstrated the ability to synthesize magnetite nanoparticles at room temperature. Finally, we utilized 3D printing to recreate the structural features within the shell of the teeth to determine their effect on abrasion resistance.

Overall objectives

The long-term objective of this project was to understand the mechanisms of nanostructural development in mineralizing environments and relate them to creating hierarchical nanostructures that afford impressive functional properties, specifically in unique abrasion resistant and damage-tolerant composites. The progress from this work will enable the development of the necessary tools for the design and fabrication of cost-effective and environmentally friendly engineering materials that mimic key design elements and performance properties present in biological systems.

We achieved this by investigating the underlying organics that direct the nucleation and fine-tuned growth of mineral using modern spectroscopic and microscopic characterization techniques. Specifically, we performed **(i)** a detailed study of the chemical and ultrastructural features of the fully mineralized radular teeth in *Cryptochiton stelleri* with a complementary mechanical investigation (combined modeling and experimental) of the mineralized structures, **(ii)** a thorough investigation of the underlying organic framework (structural and chemical) that provides templating for mineral growth as well as scaffolding for the teeth, **(iii)** synthesis of biomimetic materials through in-vitro mineralization studies to understand organic-inorganic interactions and growth mechanisms that provide architectural features that enhance abrasion resistance and damage tolerance.

We have accomplished many of these objectives, however some remain in progress. We report accomplishments by each task, specifically highlighting accomplishments in the past year.

Accomplishments of Specific objectives:

1. ***Investigation of chemical and ultrastructural features of the fully mineralized radular teeth in Cryptochiton stelleri (chiton) with a complementary mechanical investigation of the mineralized structures.***

We have utilized microscopic and spectroscopic techniques to uncover ultrastructural features in the chiton that may lead to an understanding of its remarkable mechanical properties. In order to perform examination of the fully mineralized teeth, we needed to extract the entire radula (Figure 1) from the Chiton.

Figure 1. Entire radula from the Chiton, showing the transition from non-mineralized teeth (left, white) to fully mineralized teeth (right, black).

It is clear from Figure 1 that there is a continuous transition from non-mineralized teeth to fully mineralized teeth. It is this continuous transition within this structure that may provide major contributions to understanding of development of unique mechanical properties and mineralization within this biological composite. Chemical and structural investigation of the fully mineralized teeth (the last 10 rows of the radula) highlighted a core-shell structure. Analysis of cross-sectional specimens provided a unique view of its overall architecture and its hierarchical organization. Using back-scattered SEM imaging, we were able to show the distinct core-shell structure within the teeth. However, the tip of the cusps in the teeth consisted only of the shell material (Figure 2).

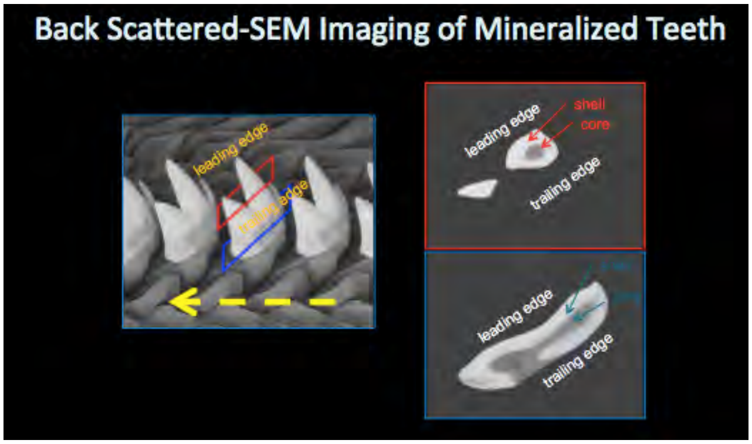

Figure 2. Back Scattered Analysis of the tip and base of the fully mineralized Chiton teeth.

Elemental mapping (Figure 3) was used to investigate general trends in composition from the core to shell of the teeth.

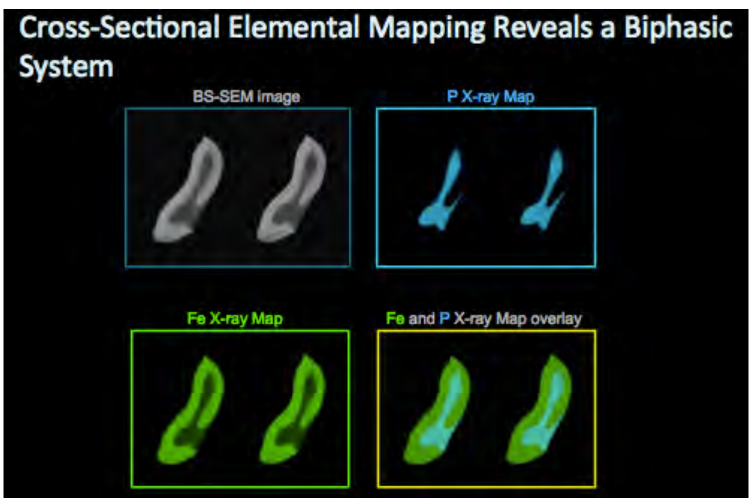

Figure 3. Energy dispersive spectroscopy (EDS) analysis of cross-sectioned samples of fully mineralized teeth revealing iron and oxygen rich shells and iron and phosphorus rich cores.

Higher resolution spot analysis with EDS (Figure 4) showed that the core region was significantly more rich in organic than the shell region and also identified the presence of minor elements (Na, Ca, K) in the core region. Based on investigation of the partially mineralized teeth and stylus (see later), we believe the role of these minor elements is for controlled transport of mineral into the core of the tooth, potentially by ion-gated protein channels.

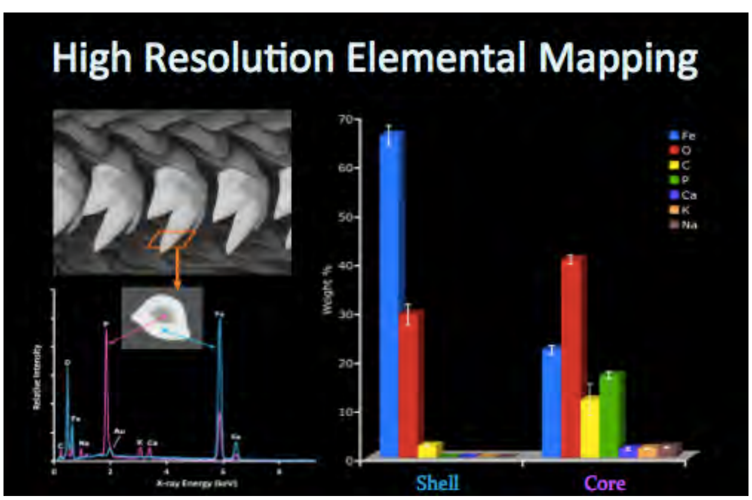

Figure 4. High-resolution EDS analysis of core and shell regions.

We performed XRD analysis on ground samples of the fully mineralized teeth (Figure 5), which revealed the presence of magnetite as the dominant mineral phase. However, we utilized Raman analysis to determine the mineral phase within the core region.

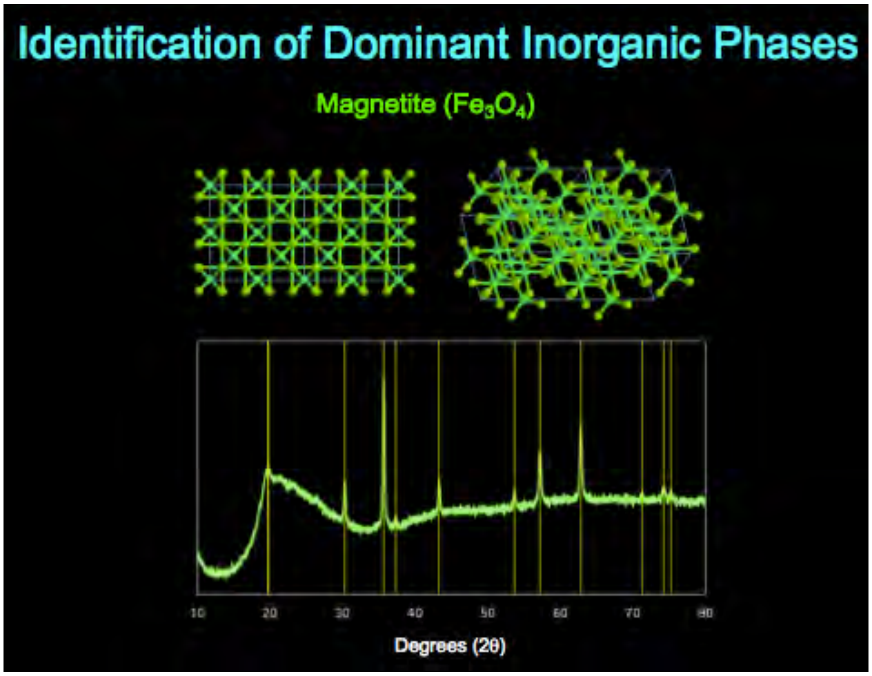

Figure 5. X-ray powder analysis of ground samples from fully mineralized teeth, revealing the presence of magnetite.

HR-TEM analysis of the shell region confirmed the presence of nanocrystalline domains (Figure 6).

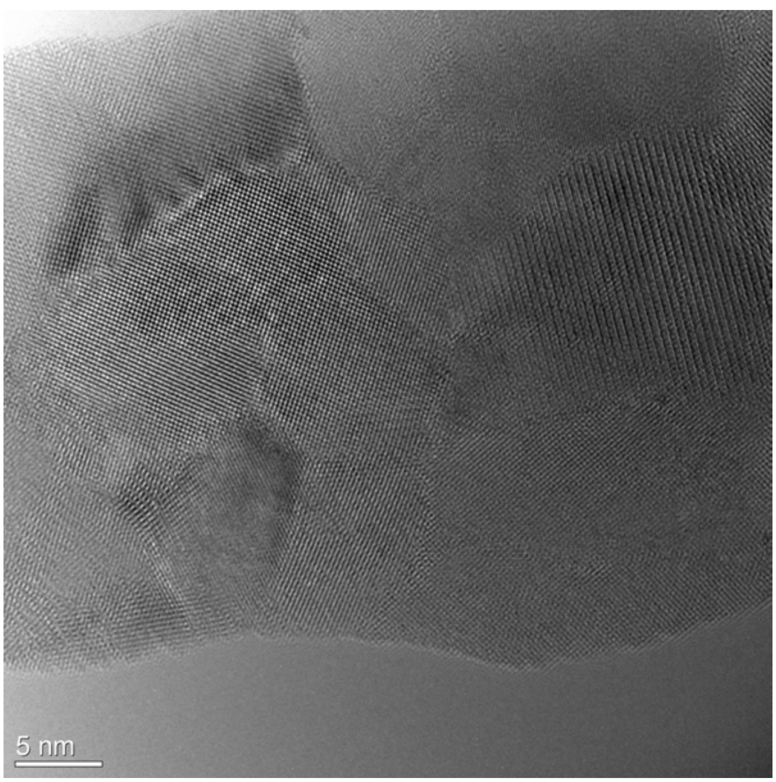

Figure 6. High resolution TEM of mineral from shell region, highlighting presence of nanograins of mineral.

Raman line scan analysis (Figure 7) revealed that the core of the tooth consisted of phosphosiderite, while the shell was formed from magnetite.

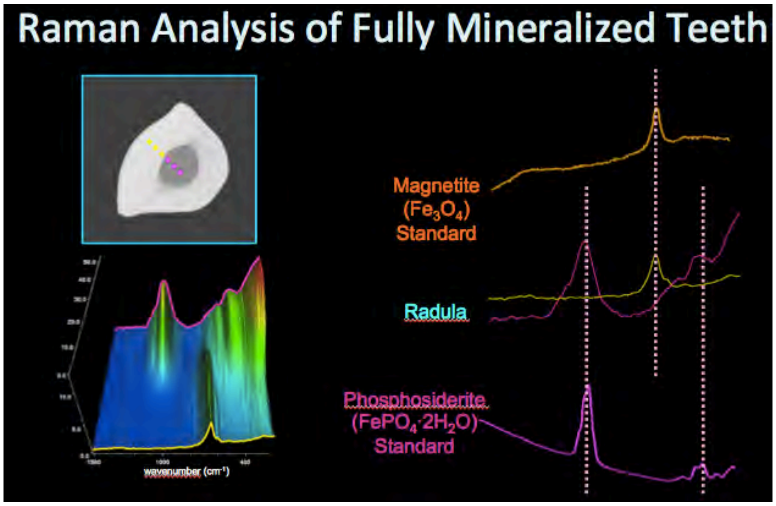

Figure 7. Line scan analysis of the core and shell regions of the fully mineralized teeth with Raman spectroscopy.

We utilized a focus ion beam technique to section the tooth in order to have electron transparent samples that could be interrogated with electron diffraction analyses. These analyses (Figure 8) in both the shell and core regions confirmed our Raman observations of a magnetite shell and phosphosiderite core.

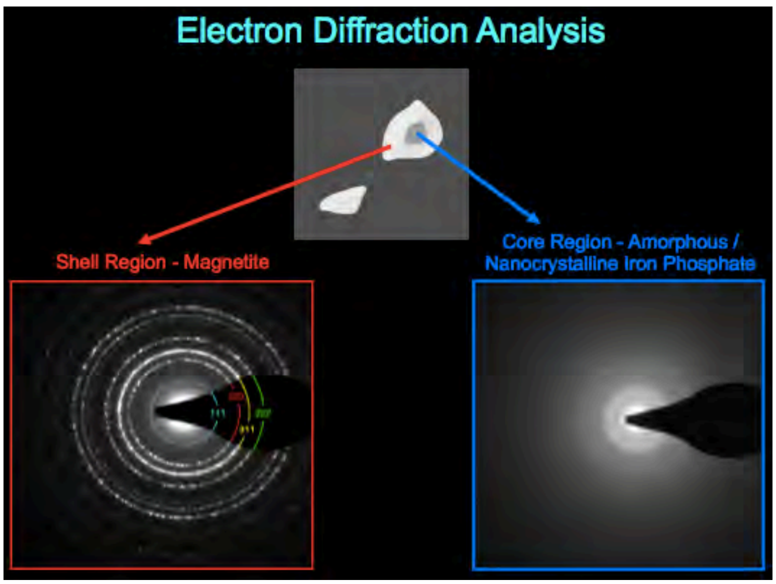

Figure 8. Electron diffraction analyses of shell (left) and core (right) regions.

Clearly, the shell region was significantly more crystalline than the core region. However, although the core region appeared amorphous, dark field imaging (Figure 9) identified that the mineral was nanocrystalline, with each grain measuring ~ 1 – 2 nm in diameter.

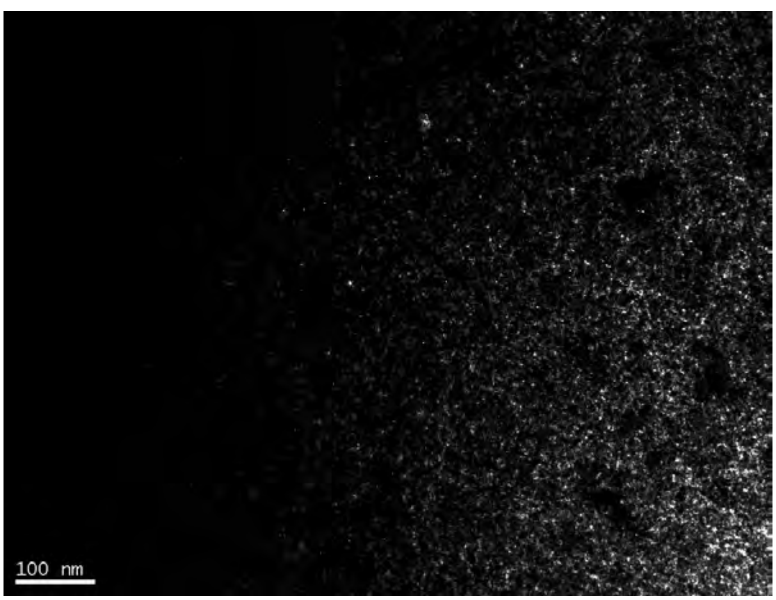

Figure 9. Dark field analysis of core region within fully mineralized teeth showing 1 – 2 nm grains of phosphosiderite.

During our analysis of the radula, we identified four separate regions of mineralization (Figures 10 - 12).

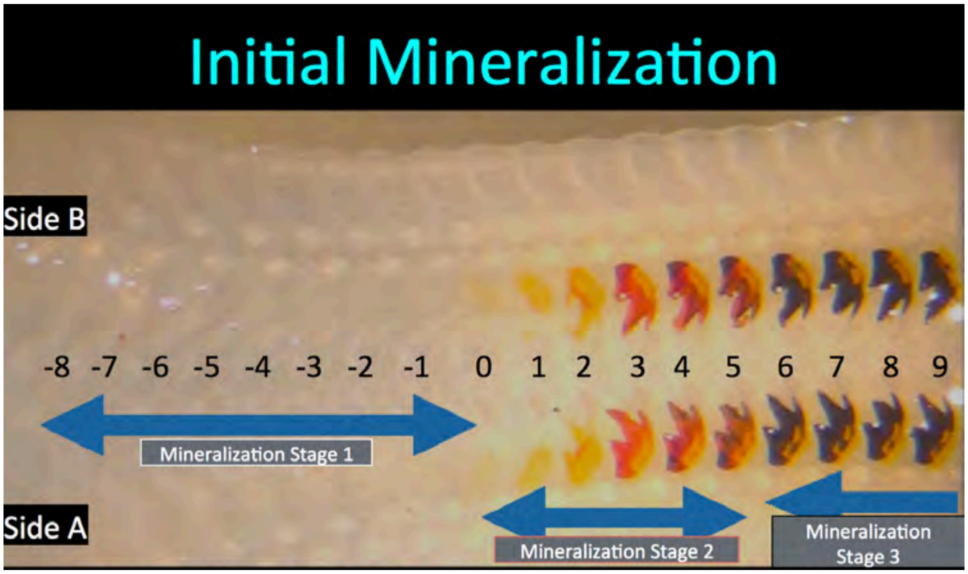

Figure 10. Initial section of the radula from the Chiton, showing the transition from non-mineralized teeth that consist of an organic framework (Stage 1) to the initial stage of mineralization (Stage 2) where Teeth are capped by a reddish brown hydrous oxide material, ferrihydrite ($5Fe_2O_3 \cdot 9H_2O$) and the Transformation to magnetite is initiated in Stage 3.

It is clear from Figure 10 that there is a continuous transition from non-mineralized teeth (Stage 1) to the onset of mineralization of ferrihydrite within the partially mineralized teeth (Stage 2). Figure 1 also shows the initiation of Stage 3, where ferrihydrite transforms to magnetite and continues to consume the remaining ferrihydrite within the shell.

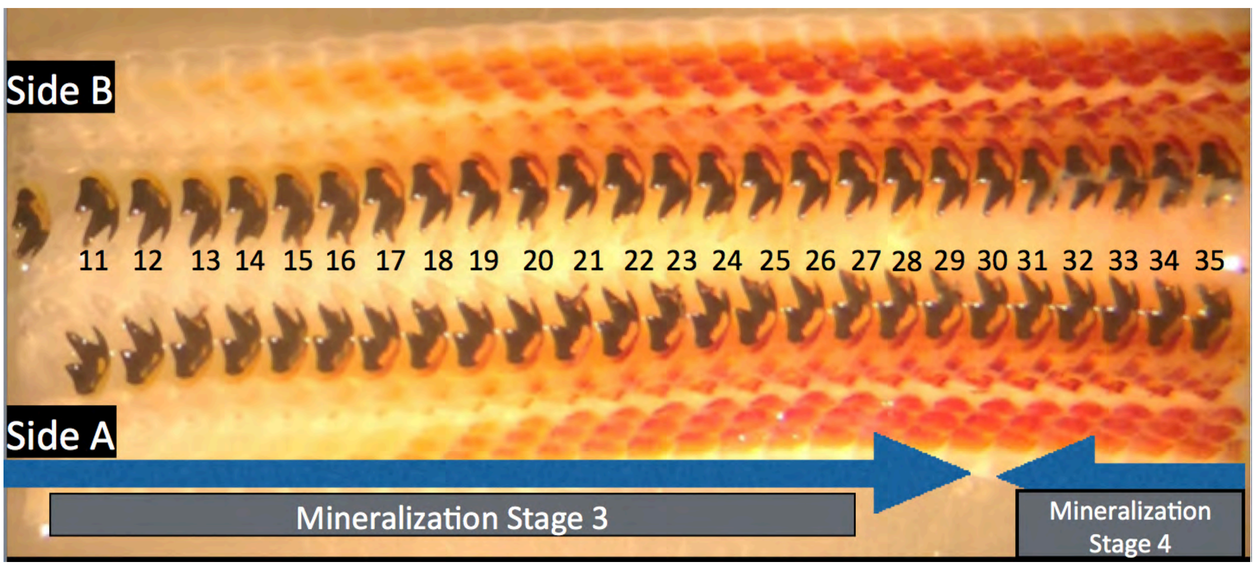

Figure 11. Stage 3 of the radula: Teeth are superficially mineralized by magnetite. Abrupt change in color from reddish brown in stage 2 to black in stage 3. Still thinly veneered by ferrihydrite. The magnetite underlying this veneer increases in thickness with increasing tooth number.

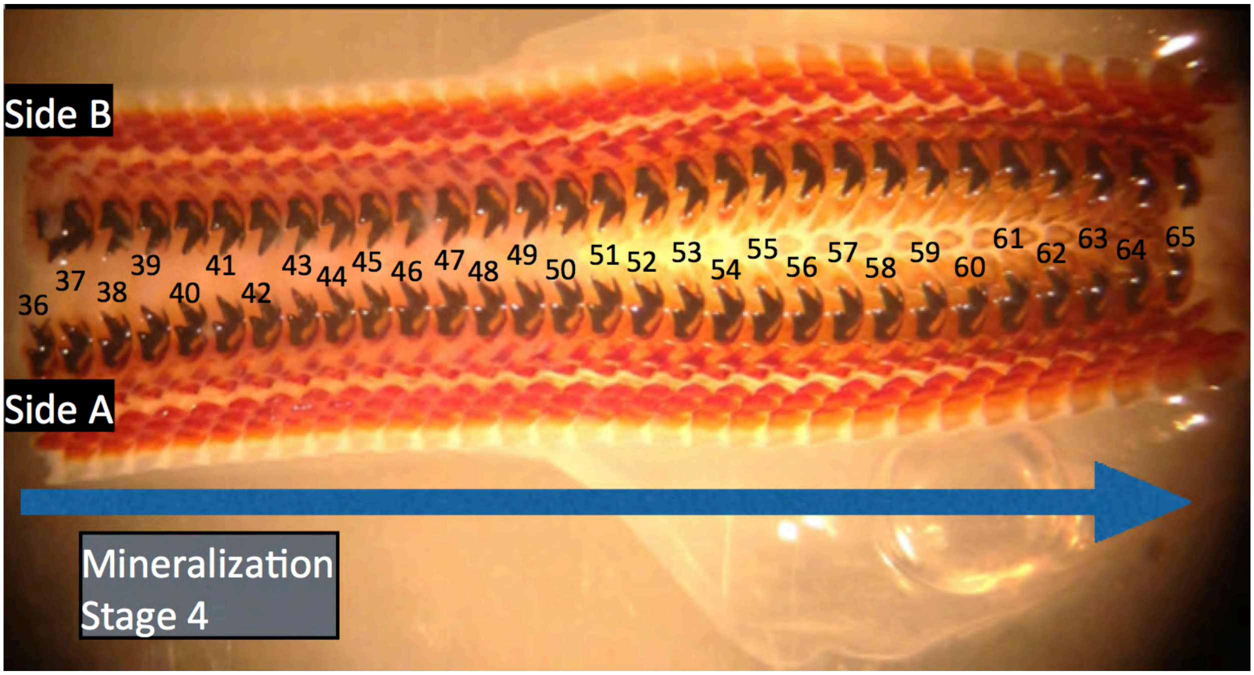

Figure 12. Stage 4: Continued thickening of the magnetite fraction in the shell, and the persistence of a superficial ferrihydrite veneer. The distinguishing feature of this stage is the infilling of the previously "vacant" parts of the tooth caps by amorphous iron phosphate.

In order to understand the underlying organic features which template the mineral growth, we produced cross-sectional and longitudinal specimens for TEM imaging. Here, we show the distinct organic fibrous structures within the teeth. However, outer region of the cusps in the teeth consisted of randomly oriented fibers, whereas regions within the shell had aligned fibers. Clearly, the scaffolds dictate final morphology (Figure 13).

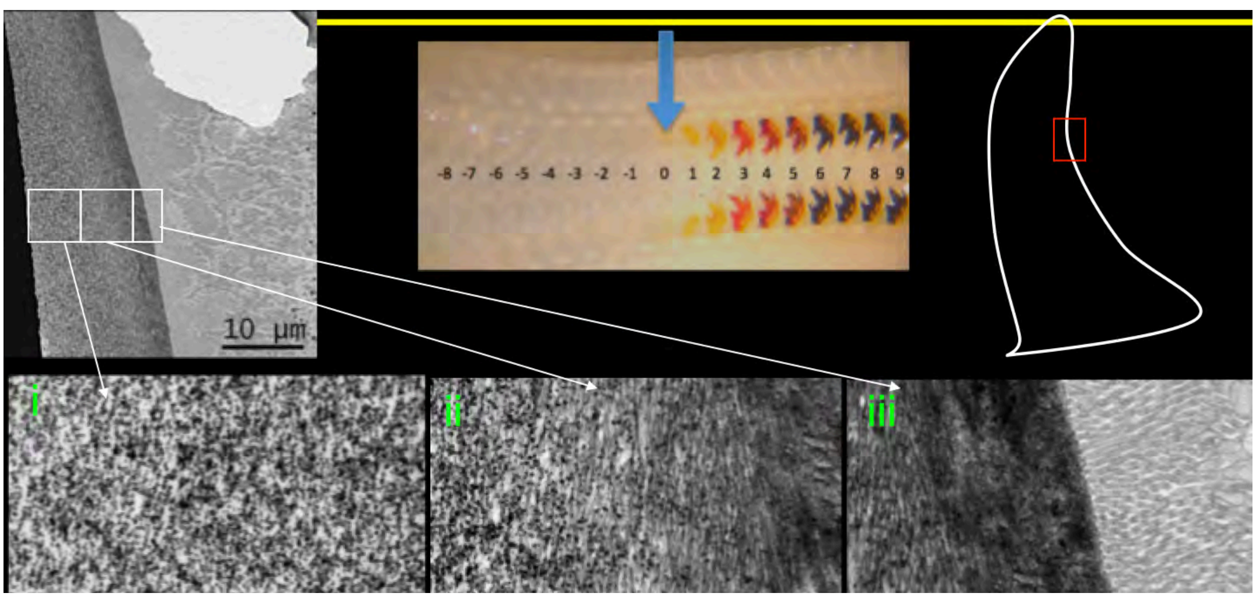

Figure 13. TEM analysis of tooth 0: Organic scaffold orientation varies within the shell of the tooth. Outer most layer (iii) consists of randomly oriented fibers whereas regions (i) and (ii) have oriented fibers.

Closer analysis (Figure 14) of the two outermost regions shows the fibrous sub-structure as well as epithelial cells that provide iron nutrient to the outermost region of the teeth.

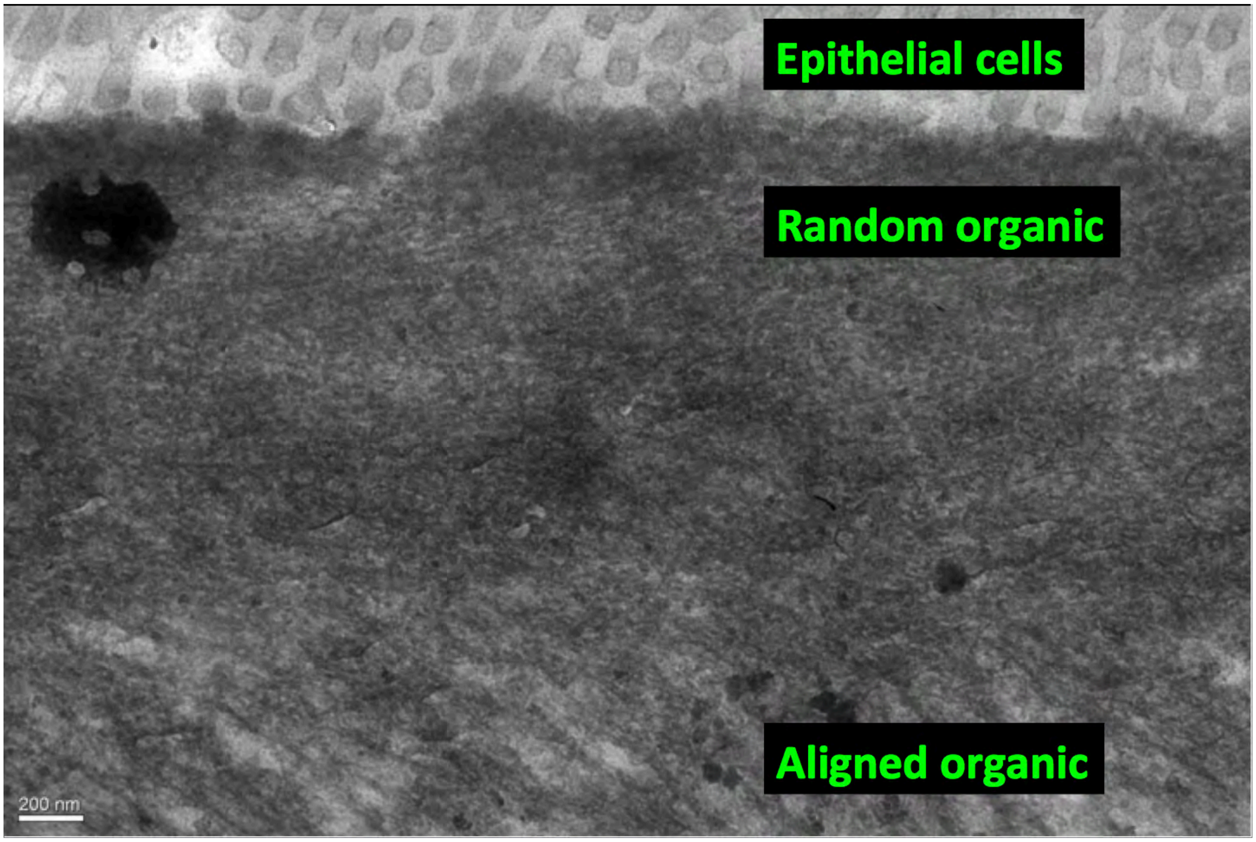

Figure 14. TEM analysis of tooth 0: Epithelial cells provide nutrient to organic that templates the mineral.

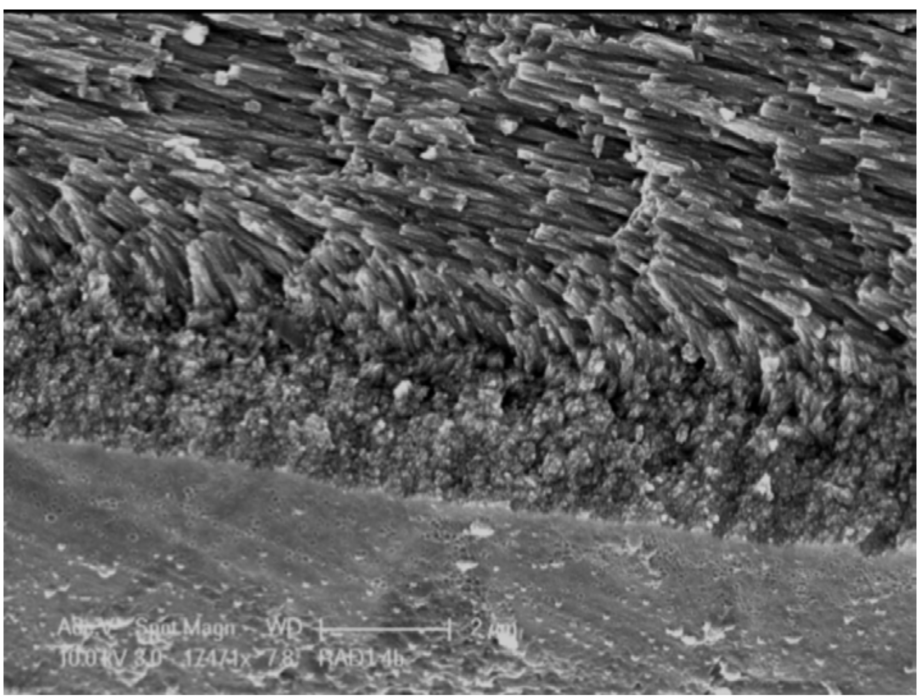

The results of this underlying organic on the resulting mineralized structures becomes clear upon analysis of the leading edge of a fully mineralized tooth (Figure 15).

Figure 15. SEM analysis of the leading edge of a fully mineralized tooth. The outermost layer consists of randomly oriented particles where randomly organic existed whereas oriented rods exist within the surface.

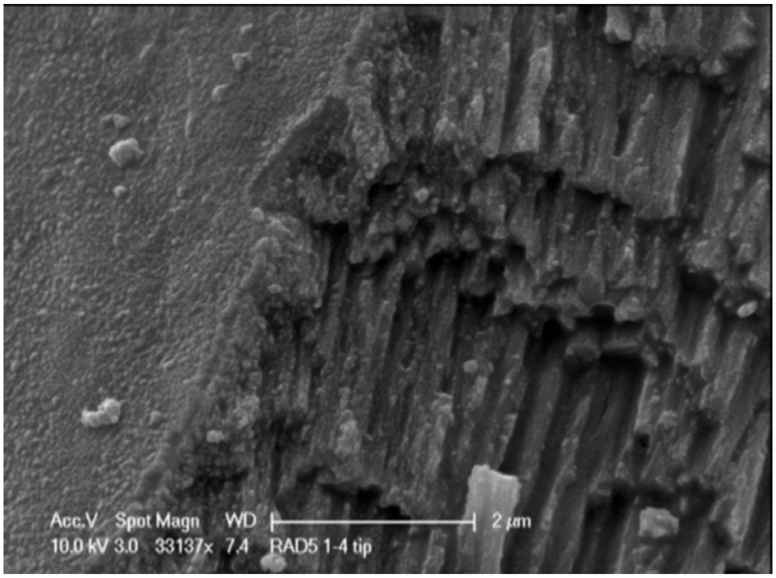

Interestingly, the trailing edge of the fully mineralized tooth does not show this particulated region (Figure 16) and the corresponding TEM from the same region in a partially mineralized tooth shows aligned organic fibers (Figure 17).

Figure 16. SEM analysis of the trailing edge of a fully mineralized tooth. The outermost layer consists of highly oriented rods.

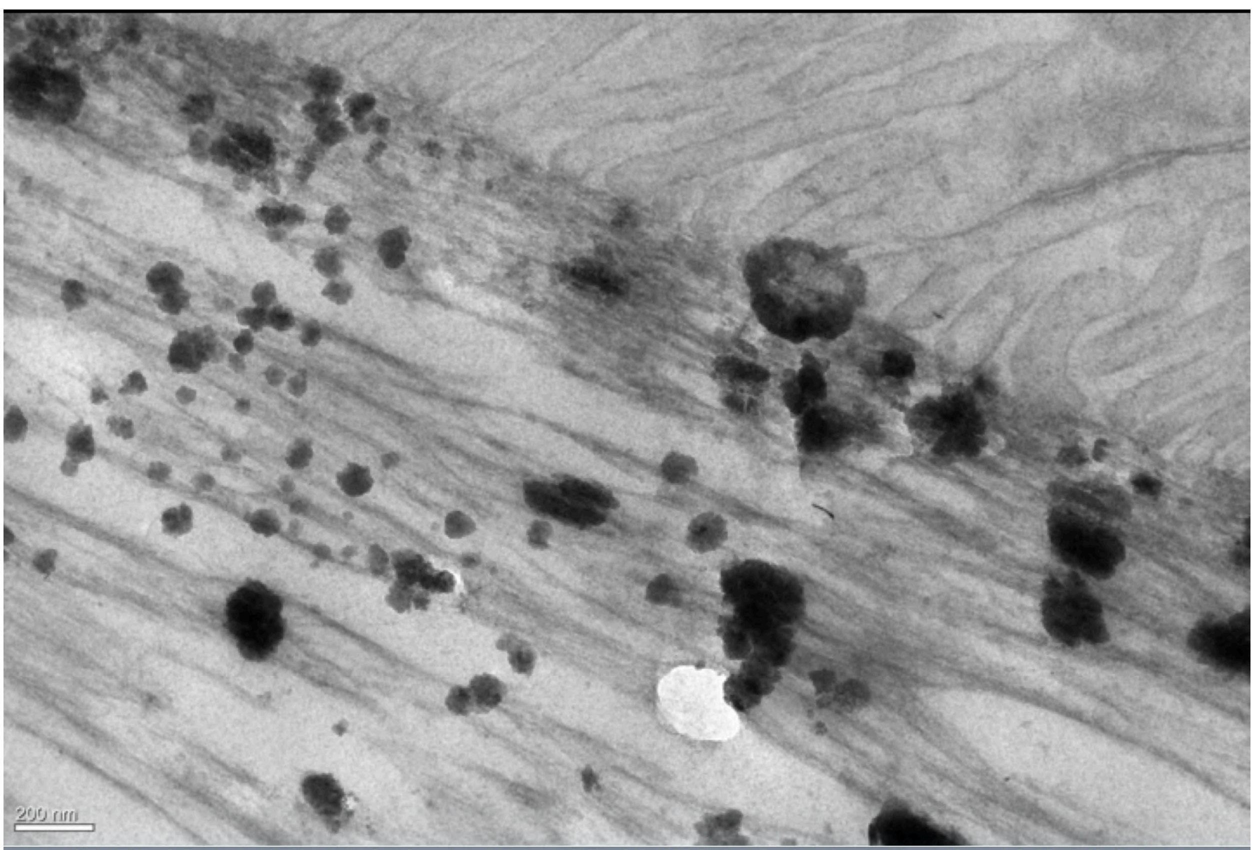

Figure 17. TEM analysis of the trailing edge of a partially mineralized tooth. The outermost layer consists of highly oriented fibers that template mineral.

In order to further evaluate the ultrastructural features within the fully mineralized tooth, a focused ion beam section was extracted from the leading edge of the tooth (Figure 18).

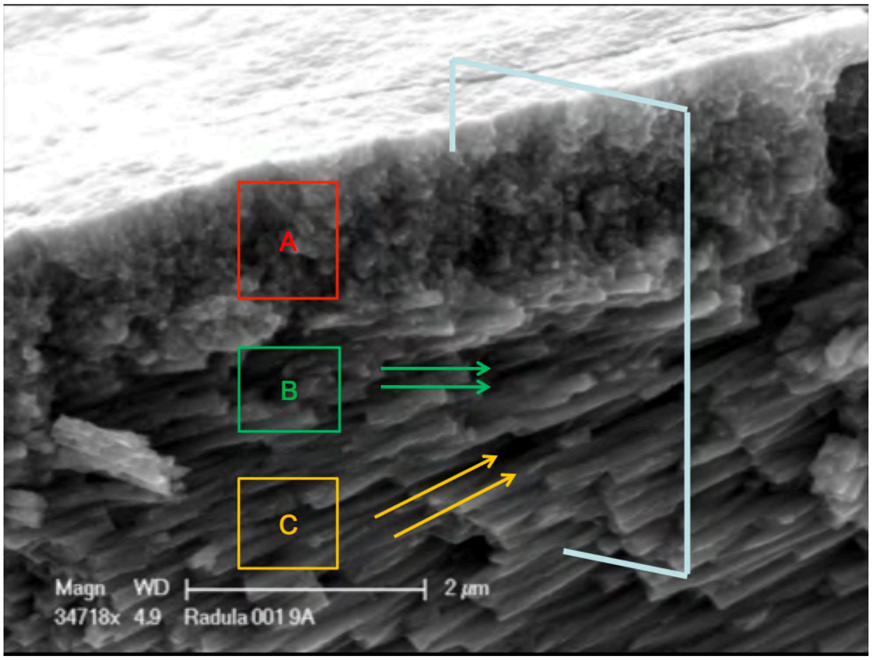

Figure 18. Region of leading edge of tooth selected for FIB sectioning in order to analyze using TEM.

Analysis from the particulate region from this section (labeled as A in Figure 18) confirms the presence of isotropic magnetite particles that are randomly packed. These particles range in size from 8-60 nm, increasing in size from the periphery inwards. Selected area diffraction and high resolution TEM confirm particles are magnetite, with no preferred orientation.

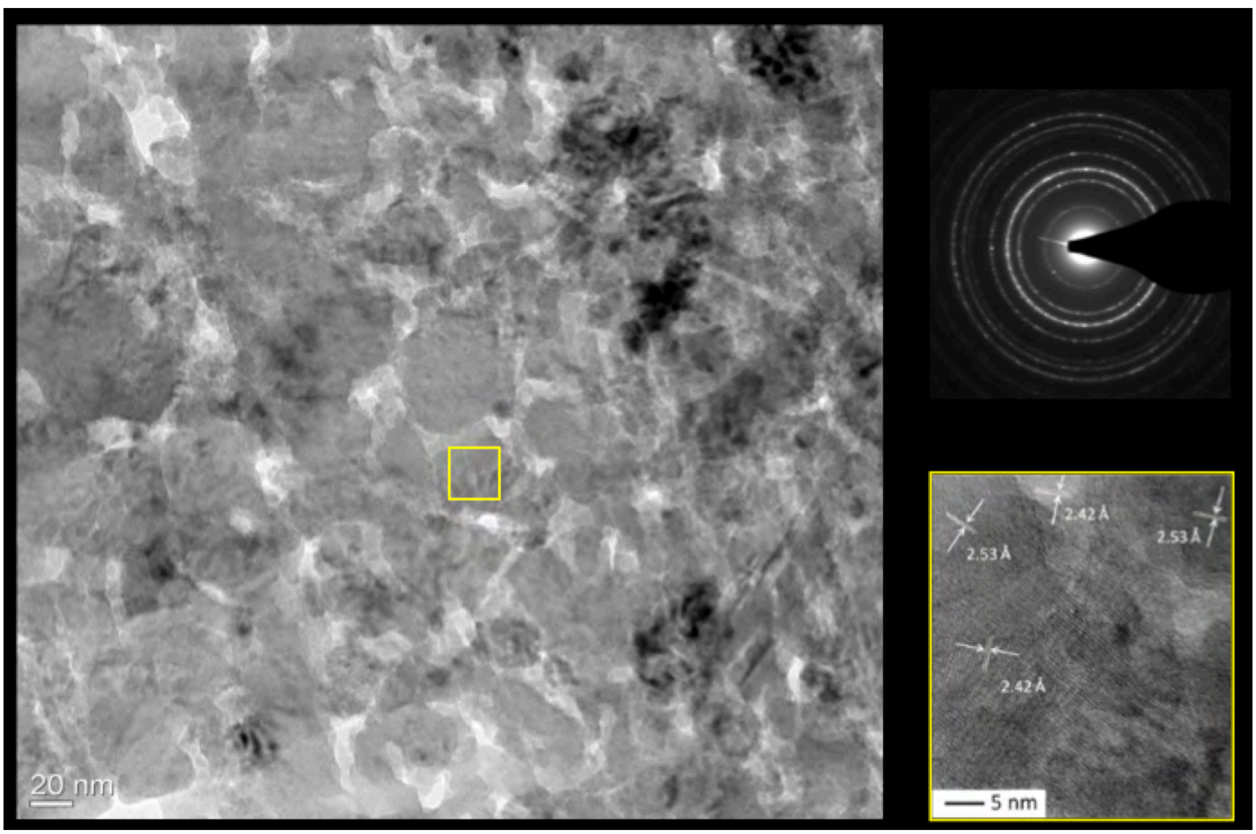

Figure 19. TEM analysis of outermost particle region of leading edge of tooth.

TEM analysis of region B from Figure 18 highlights the in-plane orientation of the nanorods (Figure 20, left) while further into the tooth (i.e., region C from Figure 18) confirms the rod rotation that is parallel to the long axis of the tooth (Figure 20, right).

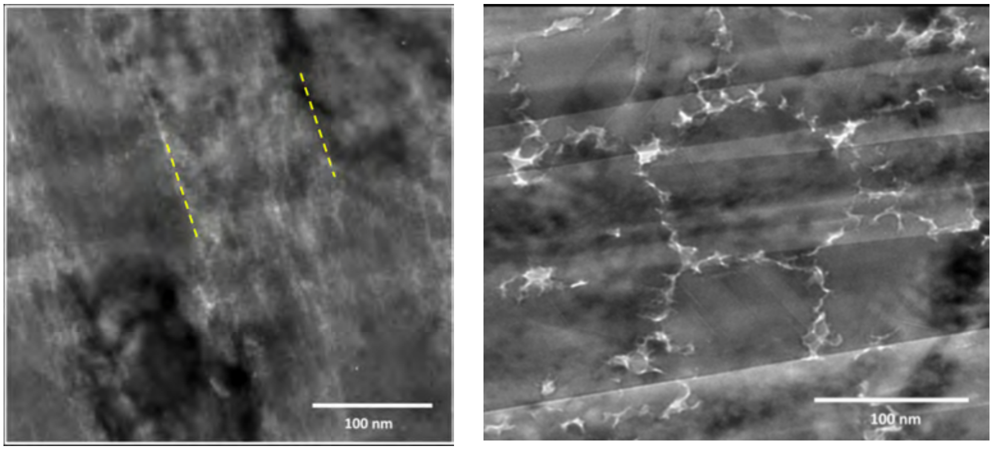

Figure 20. TEM analysis of nanorod regions of leading edge of tooth from FIB sections B and C from Figure 18.

Closer observation of region C reveals that each nanorod, which is roughened with nanoasperities on the surface, is connected to other nanorods via mineral bridges (Figure 21). This is analogous to the system observed in nacre from the abalone shell and implies that not only could the mineralization strategy be similar, but the resulting structures could have mechanical advantages (i.e., toughening) due to this processing method that yields these similar features.

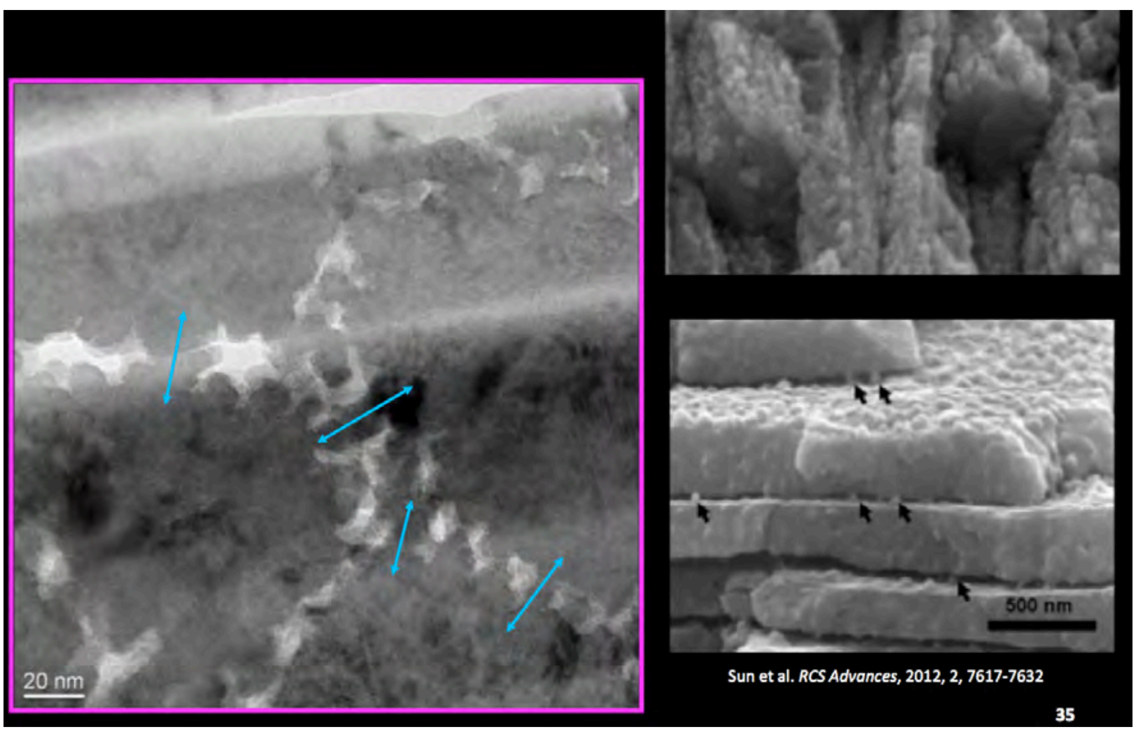

Figure 21. TEM analysis of the nanorod region from the leading edge, highlighting the presence of mineral bridges (left). SEM of the surface of the rods (upper, right) highlighting nanoasperities, which are similar to those seen in nacre tablets (lower, right).

These mineral bridges stem from the roughened morphology produced during the crystallization process, where precursor is transported not only to fiber surfaces to produce the cores of the nanorods, but excess precursor forms the surface asperities which in contact, fuse with the same crystallographic orientation. Although the mechanism has not been completely revealed, it provides some rationale to this hypothesis. Further investigation is planned.

As we continued our analysis of the mineralization within the chiton teeth, we noticed that between teeth #34 - #44, there was a continual increase in mineral being transported into the core region of the cusp. Back scattered SEM highlights this mineralization (Figure 22).

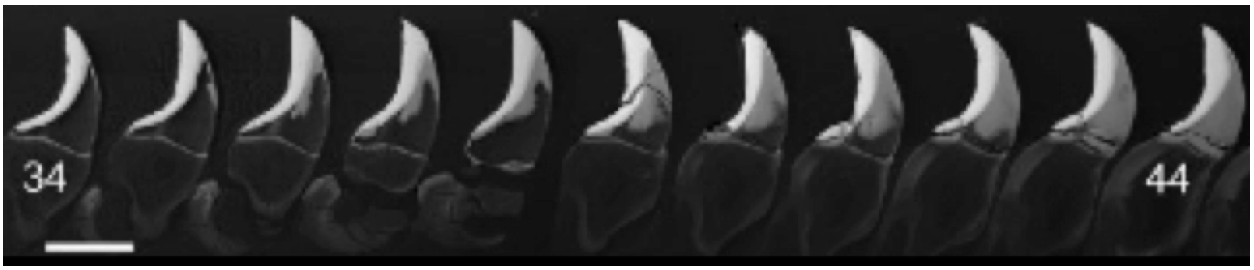

Figure 22. Back Scattered SEM of chiton teeth from row #34 - #44. Clearly the core is becoming mineralized.

EDS analyses (Figure 23) determined that this build up was of phosphorus that seems to be transported from the stylus, followed by emergence of phosphorus into the core of the tooth.

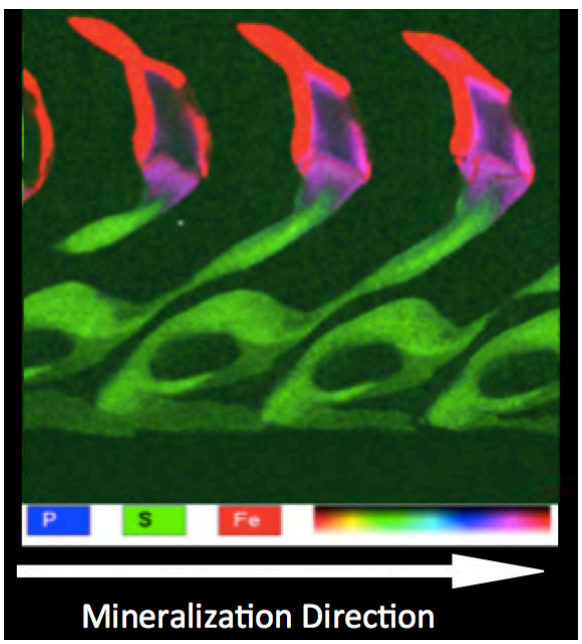

Figure 23. Energy Dispersive Spectroscopy of chiton teeth highlighting the increase in Fe and P species into the core of the tooth from the stylus.

The EDS analyses showed this insertion of Fe and P species, which based on analyses of fully mineralized teeth, was confirmed to be phosphosiderate (Iron phosphate). In addition, we note that the stylus was rich in sulfur and that this is likely to be sulfated polysaccharide that is stiffened to enable the stylus to transfer load to the tooth during rasping.
In addition, we observed prior to this mineral transport into the core, there was a concurrent buildup of both Ca and P at the interface between the stylus and core of the tooth (Figure 24).

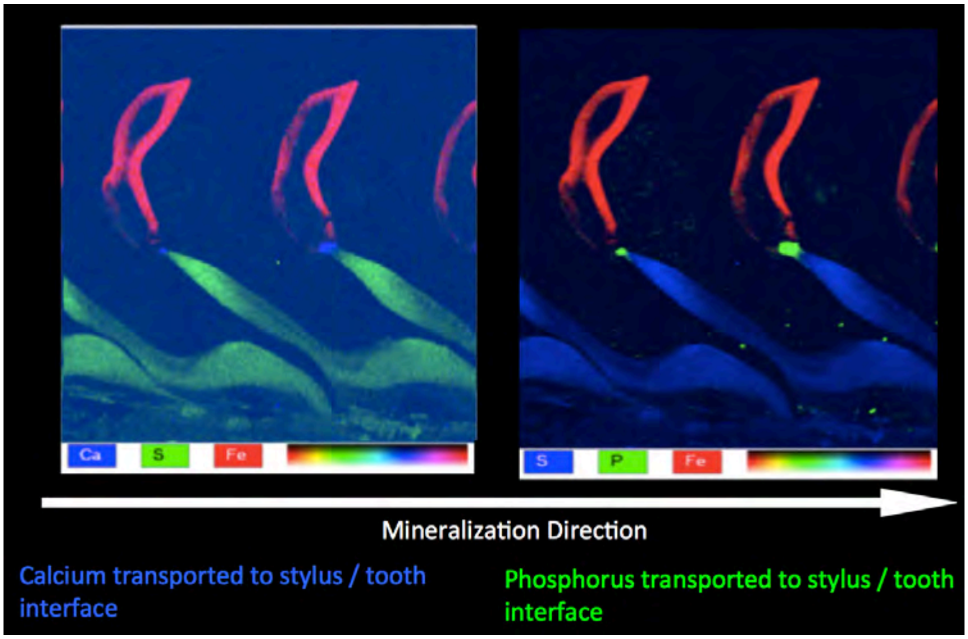

Figure 24. Energy Dispersive Spectroscopy of chiton teeth highlighting the buildup of both Ca and P at the interface between the stylus and core of the tooth.

We suspect that there may be proteins at the interface that regulate transport of PO_4^- ions into the core of the teeth. However, further analyses are required.

Using proprietary software from a collaborator at the University of Western Sydney, Dr. Ric Wuhrer, we are able to look at specific modifications in phases. Here, we plot the intensity of different elements across an entire EDS map. Then, nodes within these plots are selected and regions with those combinations of concentrations of elements are subsequently highlighted on the EDS maps.

Initially, we highlighted regions where the concentrations of sulfur relative to Fe or P were high. From this (Figure 25), we can clearly see the localization of sulfur in the stylus, suggesting the role of sulfur as a stiffening agent, either as a sulfated polysaccharide or disulfide linkages.

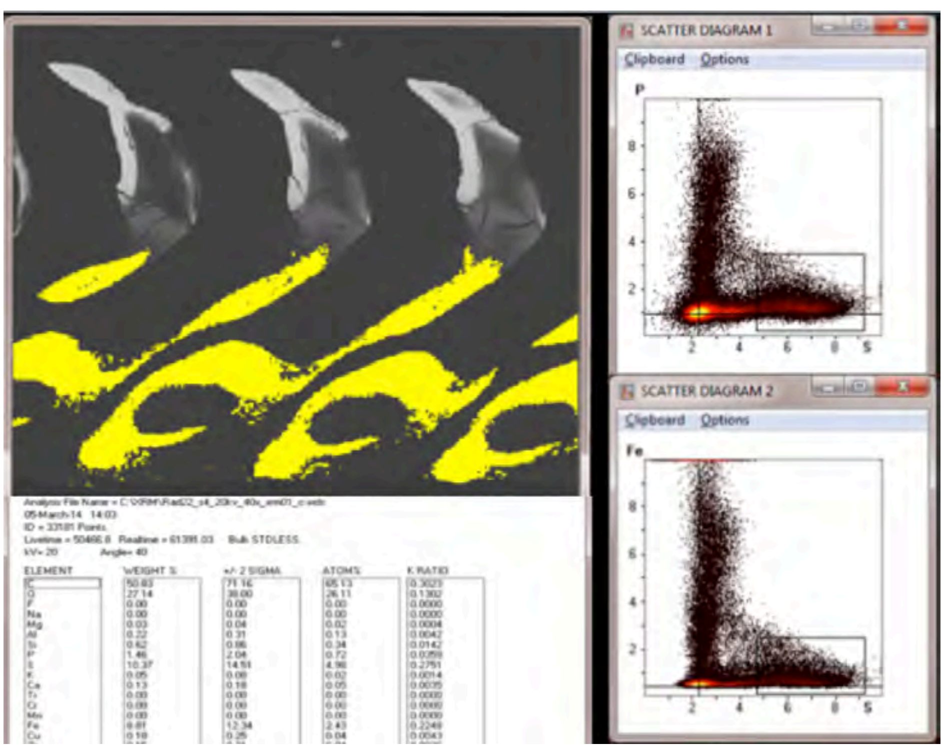

Figure 25. Energy Dispersive Spectroscopy map (left) from highlighted sulfur rich nodes (right).

Additionally, we observed trends in Fe and P across teeth in region S3 where the core was filled with mineral (Figures 26, 27). Figure 26 is at an earlier stage of mineralization than Figure 18.

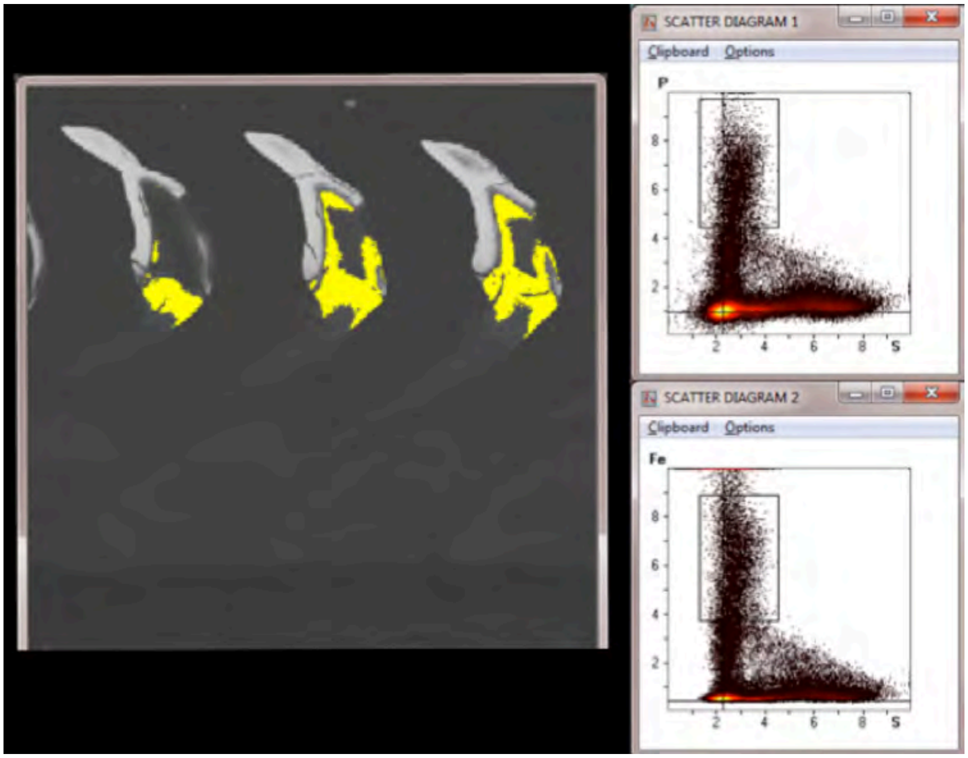

Figure 26. Energy Dispersive Spectroscopy map (left) from highlighted Fe and P-rich nodes (right) in less mineralized teeth from the S3 region.

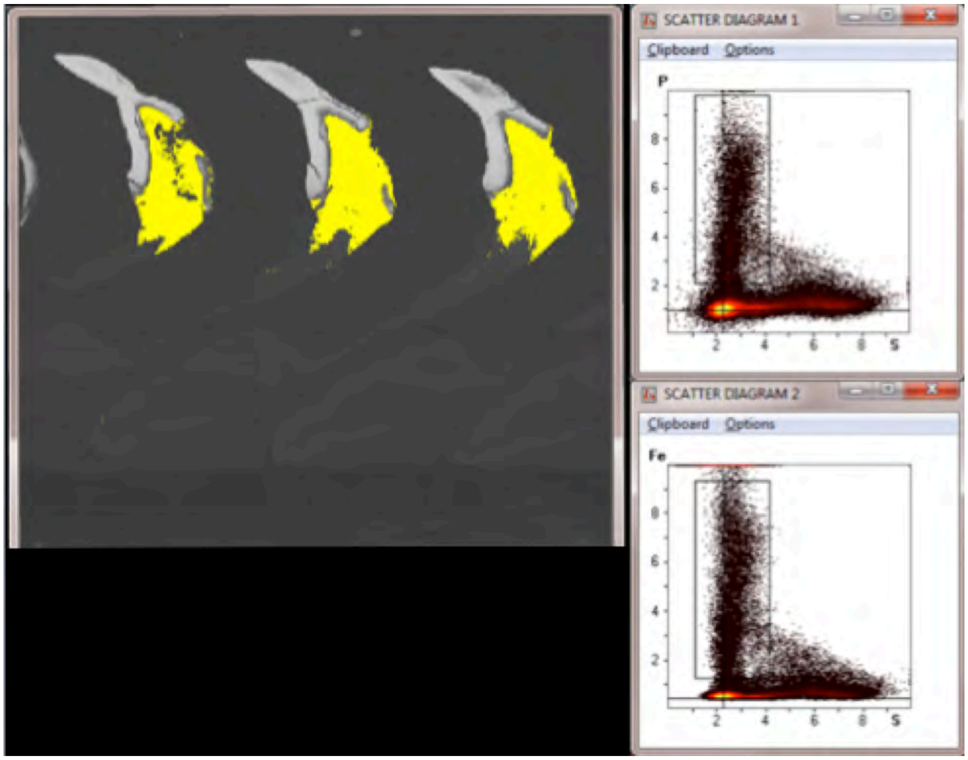

Figure 27. Energy Dispersive Spectroscopy map (left) from highlighted Fe and P-rich nodes (right) in more (vs. Figure 26) mineralized teeth from the S3 region.

Additional analyses of the teeth have revealed (Figure 28) that indeed there is a high concentration of sulfur on the leading edge of the stylus, but that the trailing edge of the stylus has a modulated amount of sulfur. We believe that this serves to control the stiffness of the stylus, which is used to transduce force to the teeth during the rasping event. However, there is much more analysis that has yet to be performed on this stylus and many unanswered questions remain such as which organics are present within that not only regulate mineral transport, but also which organics likely inhibit mineral from precipitating too soon within the stylus.

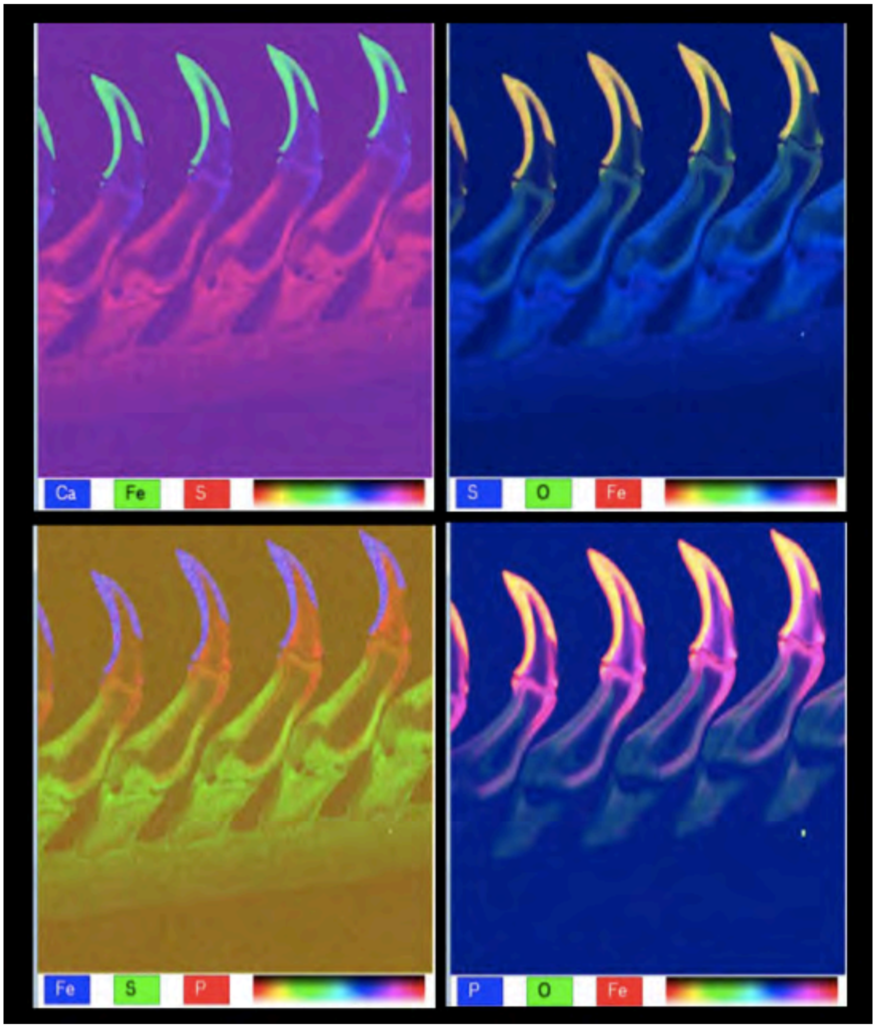

Figure 28. EDS analyses of longitudinal sections of teeth and styli within the partially mineralized teeth. The colors represent elements in the teeth.

Observations of the combinations of elements, e.g., Fe + P, the region that shows the color between the independent elements means its a mix of those elements (e.g., $FePO_4$) in that region.

Again, it is likely that sulfur, located in the stylus, provides stiffness via cross linking and that the Fe and P are likely transported into the core of the tooth along the back edge of the stylus. This work is still in progress.

Based on these observations, the internal structure of the stylus was interrogated. A stylus was frozen in liquid nitrogen and fractured along its longitudinal axis (Figure 29). Highlighted within this structure are the junction zone (with the mineralized tooth that was removed), base and a core canal. This canal may provide the stylus with the ability to transport mineral, but also allow for torsional forces to be accommodated during rasping. A closer look at this fractured surface reveals that the stylus consists of fibers that are densely packed but have varied orientations throughout its length and section (Figure 30).

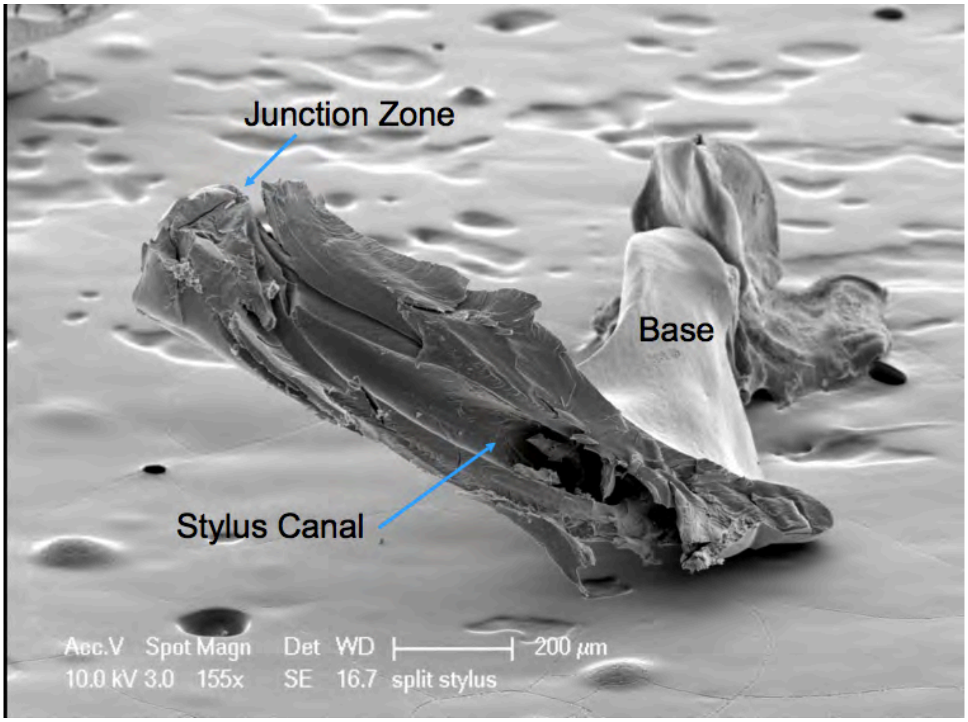

Figure 29. SEM micrograph of freeze-fractured stylus from fully mineralized tooth of radula.

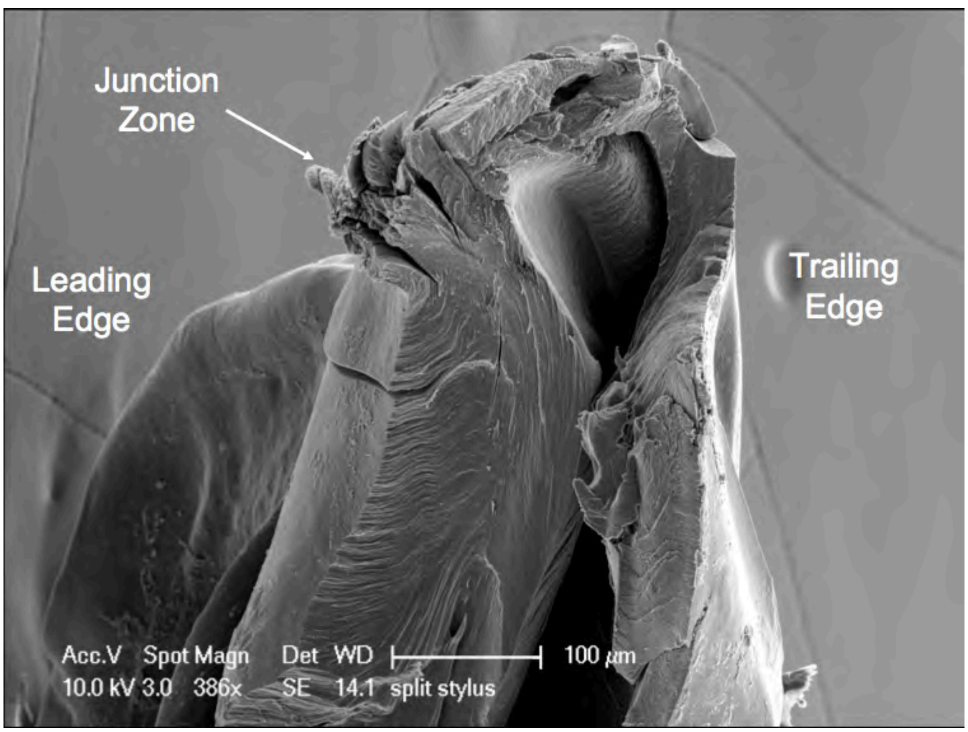

Figure 30. Higher magnification SEM micrograph of freeze-fractured stylus from fully mineralized tooth of radula highlighting leading and trailing edges as well as the junction zone with the tooth (removed during fracture).

Analysis of the fiber orientations in the leading edge (Figure 30) show that within the bulk of the stylus, fibers are aligned along the long axis. However, the fibers near the surface of the leading edge appear to rotate so that they are perpendicular with the surface. Similar observations are noted on the trailing edge, but further analyses of fiber orientation and density are needed. These fibers seem to wrap around the interior of the hollow part of the stylus ("stylus canal") and rotate in a circumferential manner (Figure 31). Again, additional analyses are needed.

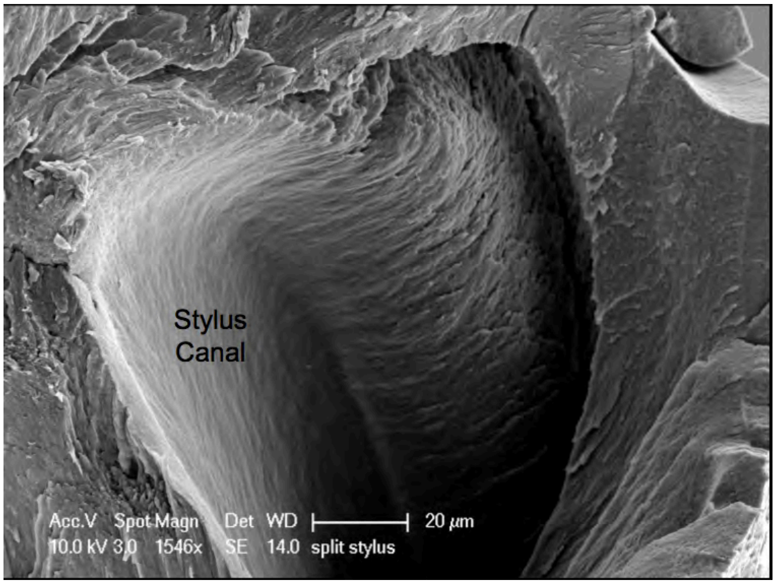

Figure 31. SEM micrograph of fractured stylus highlighting canal region.

Back scattered SEM (Figure 32) of this fracture highlights that the stylus does not seem to contain mineral phases, even though the EDS analyses show some presence of Fe, Ca, O, and P. It does reveal that there is mineral between the tooth and stylus and that this mineral seems bonded to the stylus by a thin interfacial region. Further structural and mechanical analyses are planned to understand what the components of this interface are and their role in connecting the relatively soft stylus with a dense and hard tooth to prevent failure during rasping.

Figure 32. Back-scattered scanning electron micrograph of fractured stylus highlighting mineral interface.

FTIR analyses of regions with the stylus and tooth were performed. Figures 33 – 35 show FTIR maps of the junction zone, leading and trailing edges, respectively. Analyses of the data is still underway, but it suggests that chitinous fibers may indeed be cross-linked to provide stiffness and that there are compositional changes along the length and across the diameter as well, which need to be further evaluated.

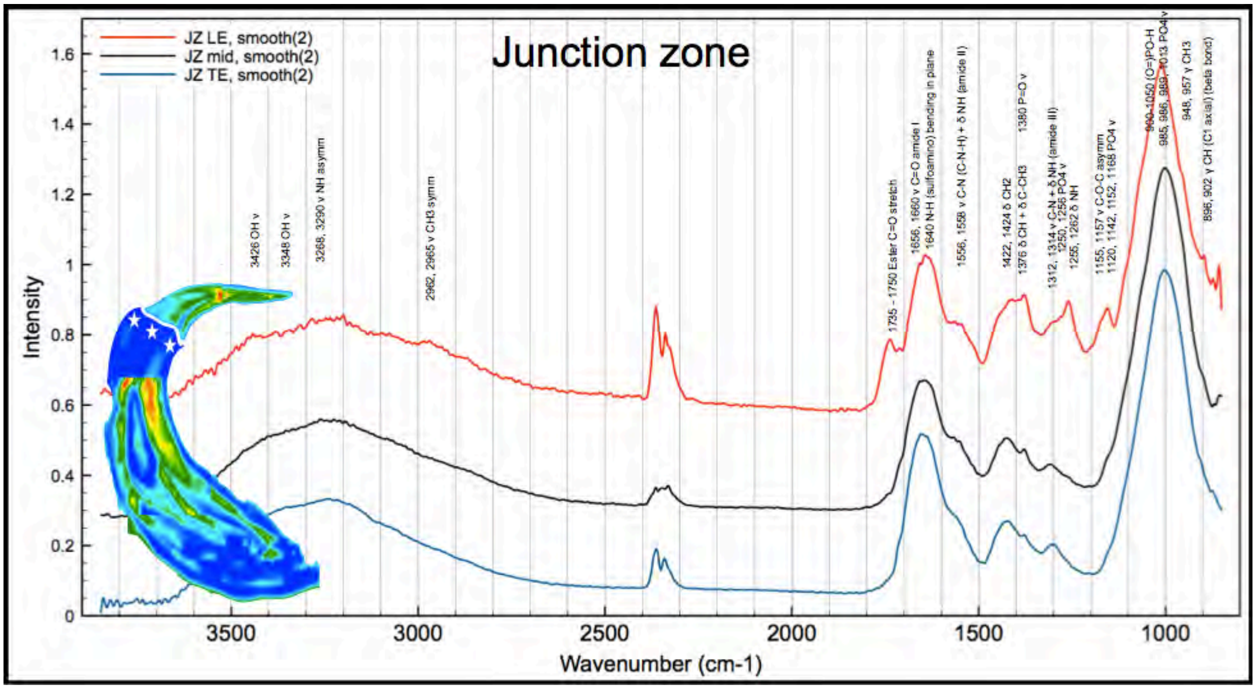

Figure 33. FTIR mapping of junction zone of tooth along leading, middle and trailing edges.

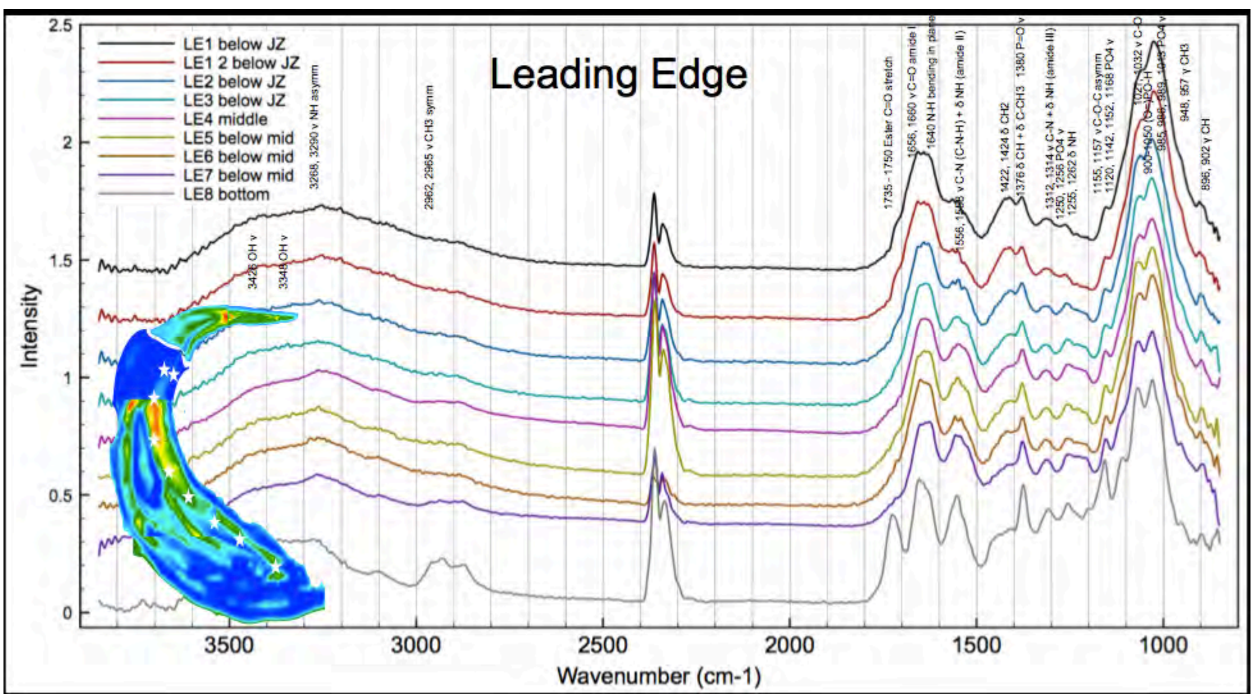

Figure 34. FTIR mapping of leading edge of tooth along length of stylus.

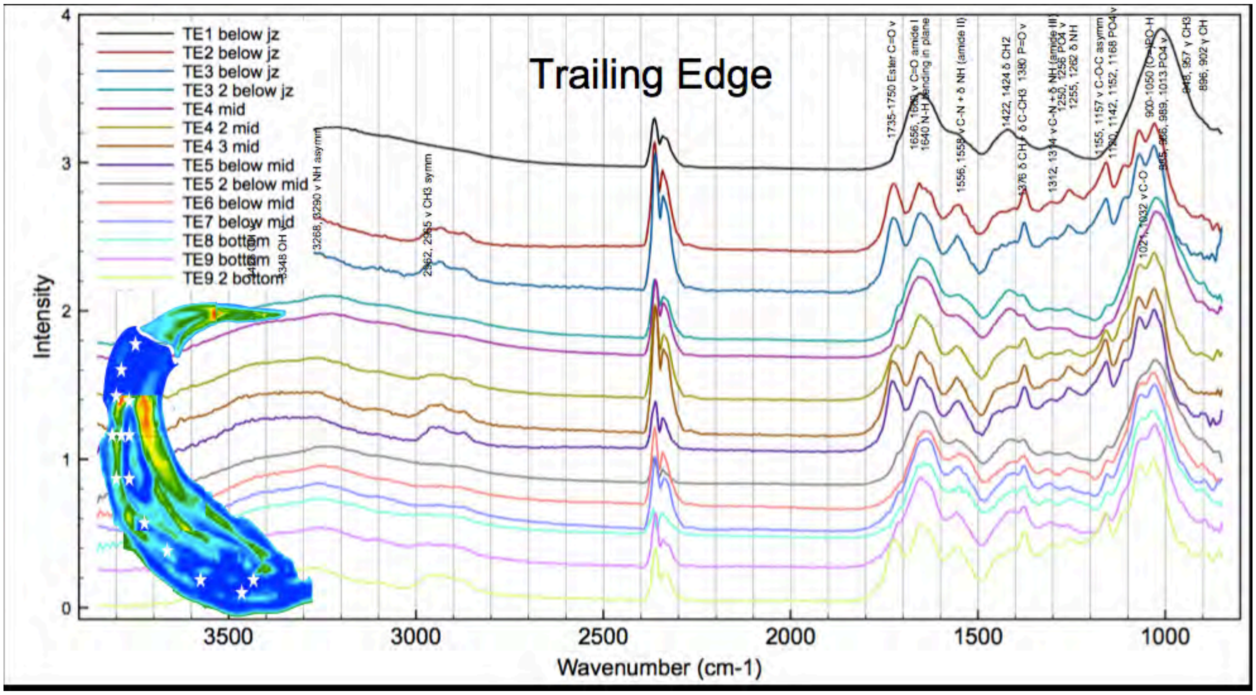

Figure 35. FTIR mapping of trailing edge of tooth along length of stylus.

Peptide-based Organic scaffold:

Here, we were interested in determining which regions of the radula have modifications in peptide concentration. We did this so that future work can pinpoint which teeth to specific target for mineral-nucleating as well as mineral precursor stabilizing proteins.

In order to do this, we removed radula and subsequently exposed them to: (i) coomassie blue protein reagent, (ii) gluteraldehyde fixation and (iii) a combination of (i) and (ii). We then observed these structures (Figure 19).

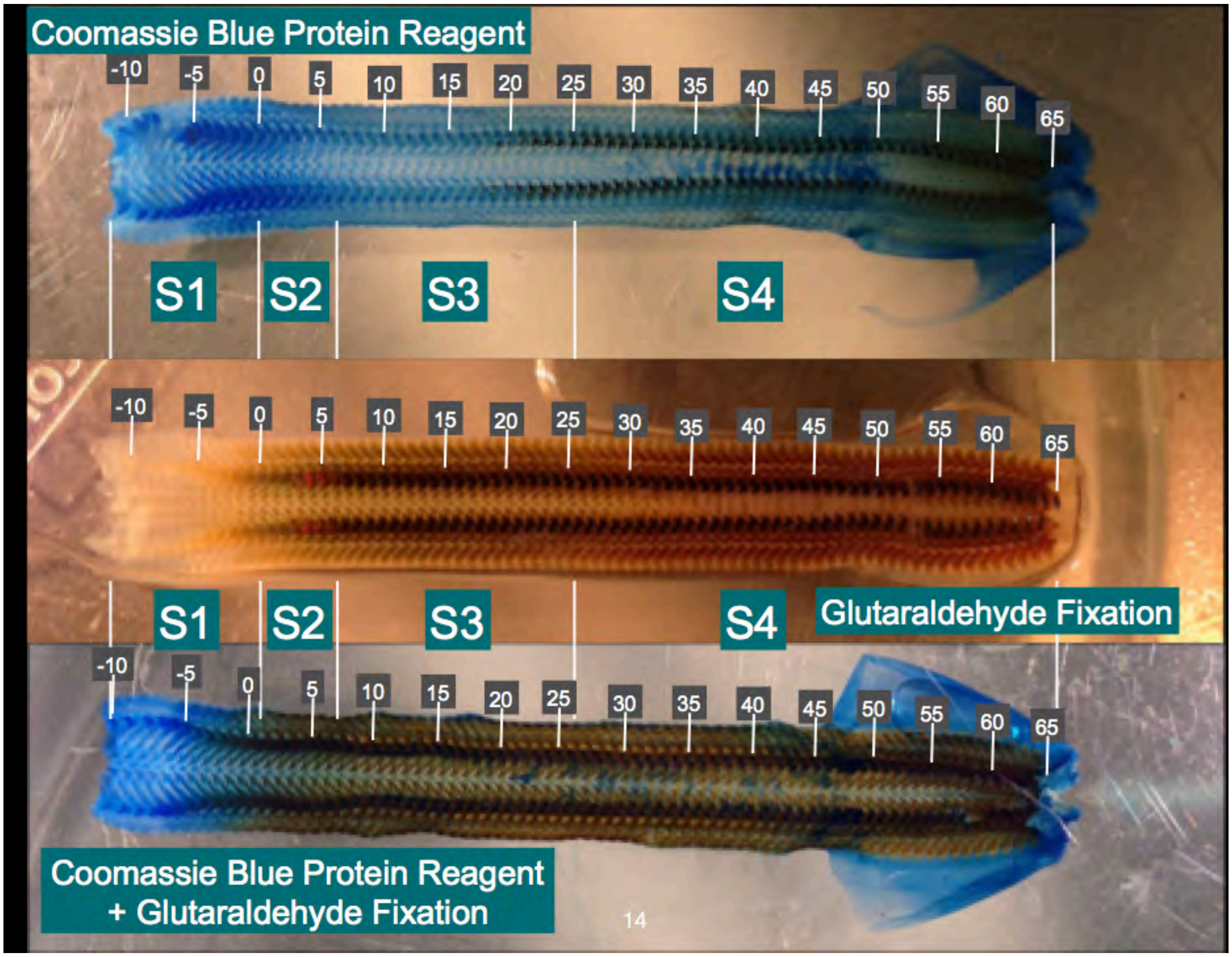

Figure 19. Optical microscopy of radula from chiton highlighting proteins in different regions.

Based on the coumassie blue staining, there is a clear build up of protein in the S1 region, especially immediately before the onset of mineral formation at S2, then falls sharply. We surmise that proteins which initiate nucleation of ferrihydrite may be present and as such, we will focus on peptide analysis in this region in future work. In addition, in region S1, we see that the first half are missing side scales, which may be the reason for the wider spacing of S1 teeth. There is a noticeable decrease in spacing in the second half of S1, along with presence of side scales. In S2, teeth #4-6 have an orange shell, but teeth #1-3 only have an orange junction zone, no orange in the shell area. Mineralization is visible in teeth #1-3 but not in the cusp. In region S3, there is a thin mineral shell that seems to be dissolved by Coomassie blue protein reagent in teeth 0-20. Finally, in S4, we observe no mineral in radular wings.

Mechanical Properties:

In addition to performing ultrastructural analyses, we attained additional mechanical performance measurements of the fully mineralized teeth in an effort to understand structure-function relationships. Utilizing our high-resolution nanoindenter, which is capable of sub-micron measurements of hardness and modulus, we observed that no rods were fractured by crack propagation (Figure 20) but rather, cracks are observed to circumvent the rods. Based on previous observations, we can confirm that the hierarchy presented in the teeth, that is, stiff-less stiff core shell structures as well as stiff-less stiff nanorods-organic sheaths provide multiple toughening mechanisms for these teeth.

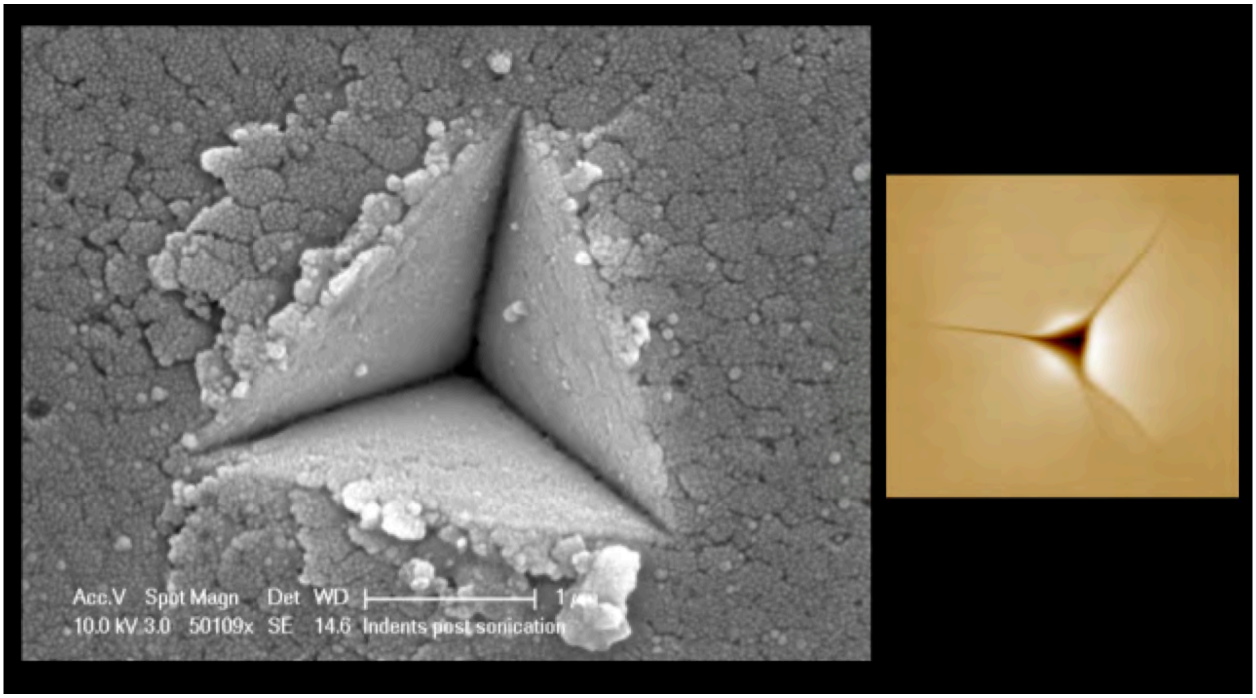

Figure 20. SEM observations of transverse section of the tooth at an indentation, revealing cracks that propagate around nanorods. The sample shown here was indented using a sharp cube-corner tip to induce cracking. After indentation, the sample was sonicated in acetone. Cracks can be seen to propagate between mineralized rods, rather than radially outward as is common with this type of indentation (shown on glass on the right).

This observation revealed that local changes in stiffness and hardness controlled fracture behavior. Specifically, that organics that may be found within or around the nanorods may redirect crack growth by controlling the energy at the tip of a crack front. In fact, in previous work, we fractured fully mineralized teeth to make local observations (Figure 21) in surface structures. Specifically, when observing nanorods, we found that fiber pull-out occurred in some regions. The fiber pull out revealed *organic material* between nanorods, as well as a *particulate covering* the nanorods and a *smooth fracture surface* within the nanorods.

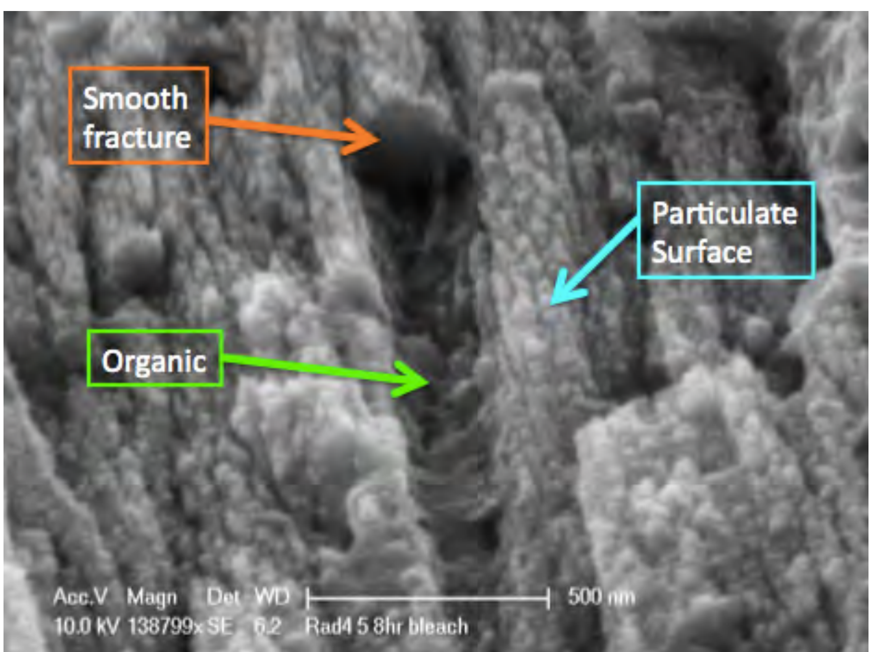

Figure 21. SEM observations of fractured region in shell with nanorod pullout that highlights

(orange), smooth fractures within rods, (green) organic around nanorods, and (blue) a particulate-like surface on the nanorods.

3. Synthesis of biomimetic materials

Based on the previous analyses, it is apparent that the organic framework both chemically and structurally mediates the formation of biomineral. We observed that the anisotropy (Figure 22) within the shell region may have an effect on the performance of the teeth. Thus, we fabricated mimics of the shell region using 3D printing of polymeric structures (Figure 23).

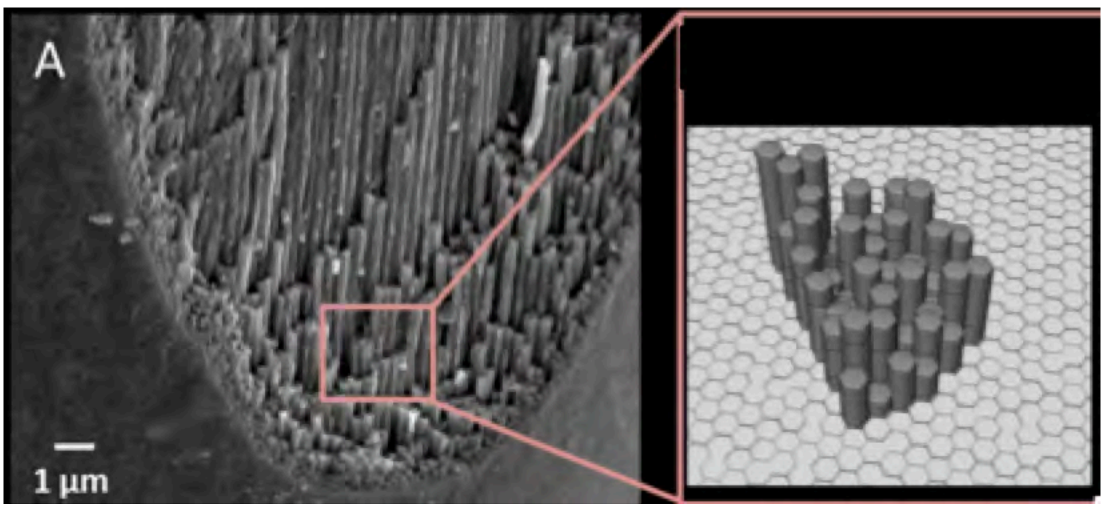

Figure 22. Rod like structure from shell region of teeth and finite element model.

We printed samples of 50mmx50mmx60mm containing around 3600 rods of 1mm of cross section. As it is difficult to measure the length of the magnetite rods in the real chiton, we tested the effect of aspect ratio in the property measured by indentation tests. The building block properties are:

Rod:
Density=1210 ± *60 Kg/m^3*
E=1954 ± 43 MPa
H= 187 ± 7 MPa

Support:
Density=1120 ± *20Kg/m^3*
E=0.93 MPa
H=0.37 MPa

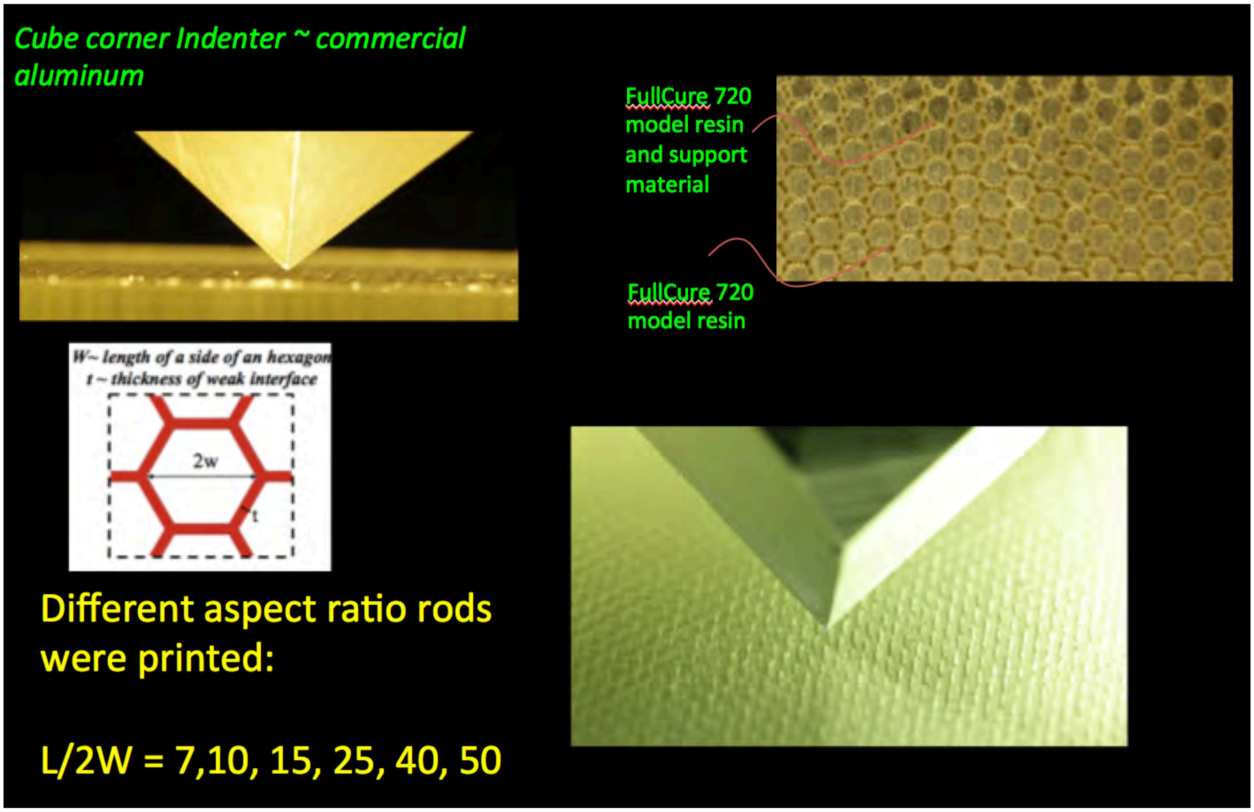

Figure 23. 3D printed mimics of shell region of chiton teeth. Samples were made with different rod aspect ratios (Length / 2 x width): 7, 10, 15, 25, 40, 50 and indented to determine optimized aspect ratio for abrasion resistance.

From this, we tested rods parallel and perpendicular to the indenter to quantify the effect of rod orientation in the mechanical properties. Based on the results, we see a number of energy dissipation mechanisms (Figure 24). Even with the difference in the hierarchical structure and composition, the biomimetic designs are able to replicate the energy dissipation mechanisms exhibited in parallel HAP crystallites of human enamel, where the support material resembles the organic sheath (proteins and collagen) of the tooth that debonds surrounding the rods.

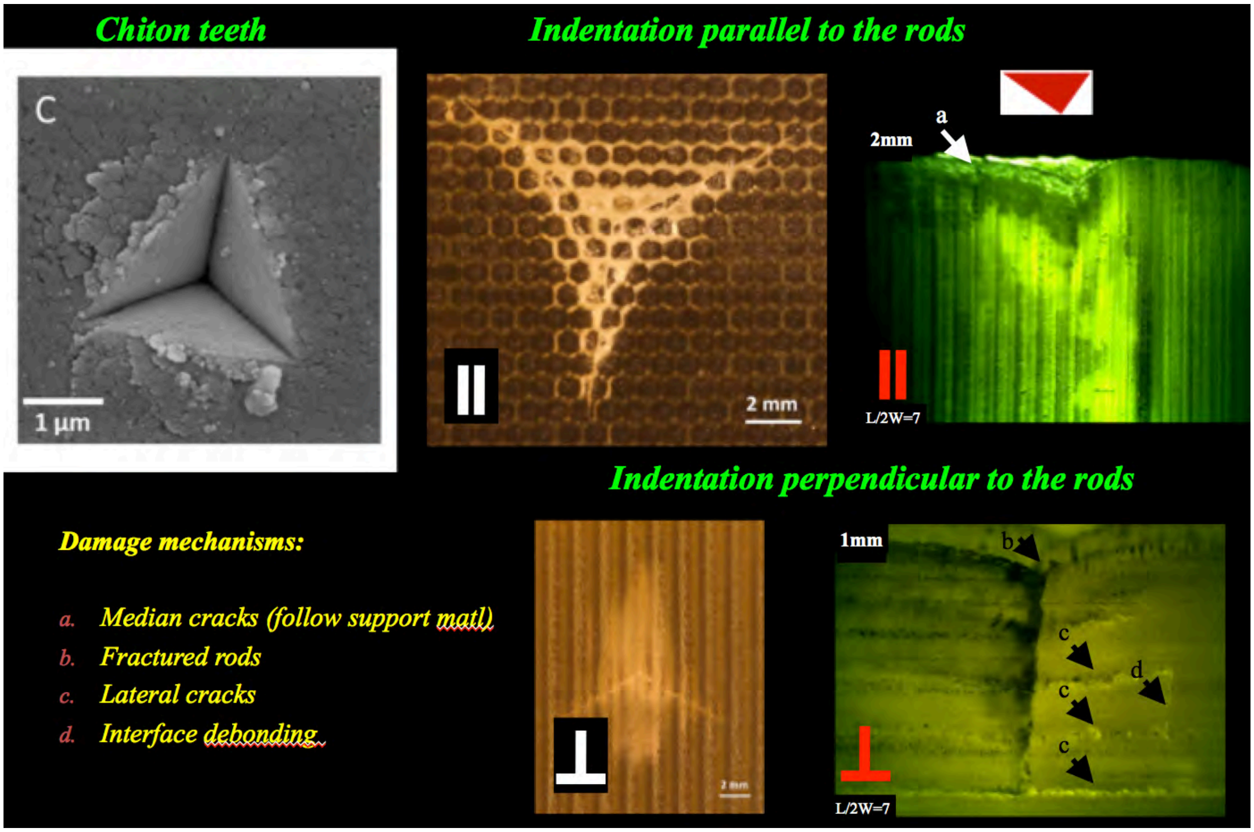

Figure 24. Results of indentation tests of biomimetic chiton teeth shells.

As compared with the parallel rod alignment, examination of the perpendicular rods reveal a preferential crack path through the solid and interface material. These characteristic mixed-modes of energy dissipation, opening and in-plane shearing, affects the fracture toughness of bio-composite materials. Although the sliced cuts limit the complex crack tortuosity displayed, experimental observations suggest that crack deflection within the weak interface layers is the preferential path for energy dissipation, preventing in this way catastrophic failure. We are now utilizing electrospinning to produce biomimetic fibers that will be assembled into hierarchical composites. These fibers will contain functionalities that will be mixed with iron-based precursors to look at nucleation and growth of ferrihydrite and magnetite.

Future Work

In the following year, we plan to investigate:
1. Stylus:
A. We want to perform a more detailed structural analysis of the macro and microstructure within the stylus. Specifically, we will look at its hierarchical assembly using high resolution microscopy as well as spectroscopy.
B. Utilize non-mineralized teeth as templates for in-vitro mineralization of iron oxide, looking at the effect of the maturity of the non-mineralized teeth on the nucleation size and density of iron oxide mineral. We will combine this with IR studies to see if the surface functionality of the fibers is changing, and if that interface controls the mineral formation.

2. Partially mineralized teeth:
A. We will continue to investigate the mineralization in partially mineralized teeth to determine how fully mineralized rods form. Specifically, we want to look at how the surfaces of the mineral particles fuse and how that relates to the toughening in the tooth.

3. Biomimicry:
A. Utilize electrospinning to produce biomimetic fibers that will be assembled into hierarchical composites.
B. These fibers will contain functionalities that will be mixed with iron-based precursors to look at nucleation and growth of ferrihydrite and magnetite.

Supported Personnel and Collaborations:
<u>Training, Education, and Outreach Achievements</u>

Training, Education, and Outreach Achievements
UCR:

- Dr. Lessa Grunenfelder (Ph.D., USC) was a post-doc working on the project for 6 months.
- Mr. Steven Herrera (BS, UC Riverside, Undergrad, Hispanic), was an undergraduate and then Ph.D. student working on the project.

Mr. Jeff Geiger (Undergrad, Male). We have had more than 10 groups of high school and community college students tour our lab in the past year.

Tokyo University of Agriculture and Technology:
Dr. Atsushi Arakaki is a collaborator in this project and an expert in molecular biology.

University of Western Sydney:
Dr. Ric Wuhrer is a collaborator on this project and an expert in Energy dispersive spectroscopy.

Finally, the PI organized and hosted an outreach event at the Riverside Metropolitan Museum in May, 2014. Here, 8 of my 11 undergraduates working in the Biomimetics and Nanostructured Materials Lab presented their research to a public audience. Undergraduates worked with middle school students in Riverside County to co-present at the museum. We built a mobile seawater system to bring our different organisms to the museum. This event has received a lot of press and has provided a lot of exposure for our students. The result of this event was a success. As with the last year, the museum reported that on average, they receive 30 – 40 visitors to their Nature lab on a Saturday afternoon (1pm – 4pm). During our exhibition, the Nature lab received over 150 visitors. These visitors included a broad diversity of the public sector including Asian, Caucasian, Hispanic males and females of a wide range of ages (3 – 70).

The program for this event is shown below:

Publications:

"Stress and Damage Mitigation from Oriented Nanostructures within the Radular Teeth of *Cryptochiton stelleri*," L.K. Grunenfelder, E. Escobar de Obaldia, Q. Wang, D. Li, B. Weden, C. Salinas, R. Wuhrer, P. Zavattieri and D. Kisailus, *Adv. Funct. Mater.*, **24** (39) (2014) 6093-6104. **(Cover Issue).** DOI: 10.1002/adfm.201401091

Two additional manuscripts in preparation.